## 2.4 SEISMIC REHABILITATION OF EXISTING REINFORCED CONCRETE AND MASONRY BUILDINGS WITH METAL-BASED SOLUTIONS

Romania is a country of moderate to high seismic risk. The first compulsory seismic design code was issued in 1963. The RC structures built before 1963, were designed to resist only gravity loads, mainly. Later, new codes were drafted (e.g. 1978, 1992, 2006) the last one being aligned with Eurocode 8. Practically, almost all the buildings located in severe seismic zones and gravity load designed must be evaluated and strengthened.

### 2.4.1 STRENGTHENING OF R.C. FRAMES WITH BUCKLING RESTRAINED BRACES

A "typical" RC frame designed and built according to the technical regulation of 1950-s is first evaluated and, after, strengthened with an inverted V BRB system. The BRB system is applied in the middle spans of the frame. Additionally, FRP local confinement of the columns was considered (see Figure 101). The confinement was applied only on the columns from the first two stories. The analysis was performed on RC frame strengthened by means of BRB with/without fiber reinforced polymers (FRP) confinement. BRB are designed to resist and provide the necessary ductility to the frame. In order to check their effectiveness and the correlation with numerical model assumptions the BRB members have been tested. The frame geometry and cross sections are presented in Figure 101.
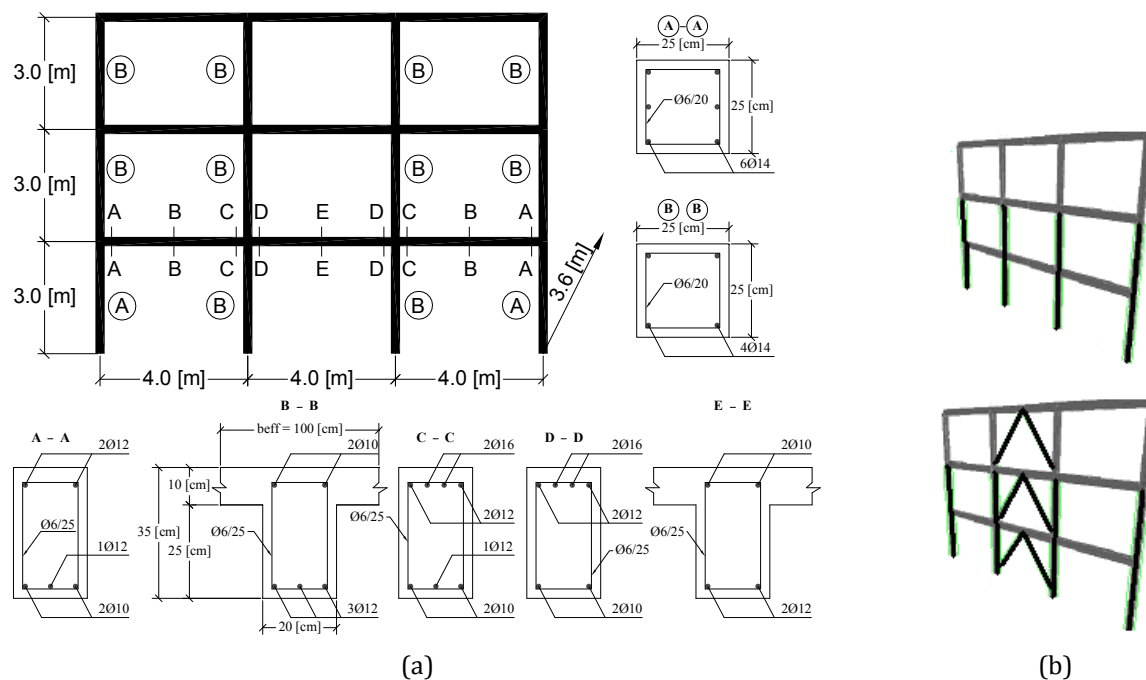


Figure 101. Frame geometry, characteristic beam and column cross-sections (a) and strengthened solutions applied on the frame (b).

Considering an inappropriate detailing of RC elements, concrete was taken as unconfined according to FEMA 356 (2000). The material model Kent & Park from Park & Paulay (1975) was considered as an unconfined material with linear softening of rigidity and no tension. Due to the poor anchorage length of the bottom longitudinal reinforcement in the beams, the equivalent yield strength of the steel was used (FEMA 356, 2000). The reinforcing steel was defined as uniaxial bilinear material of strain hardening according to Eurocode 3.

The effective stiffness of the members, corresponding to cracked cross-section, was reduced according to FEMA 356 (2000). For plastic analysis, beams and columns were modelled using concentrated plasticity at the ends, defined by a rigid plastic bilinear moment-rotation relationship. The plastic hinge length ($L_p$) was computed according to Paulay and Priestley (1992).

BRB's were considered pinned at the ends. Inelastic behaviour was modelled by concentrated plasticity. The material used for BRB is S235 grade mild carbon steel. In order to obtain the adjustment of the design strengths (maximum compression strength $C_{max}$ and maximum tension strength $T_{max}$) the AISC (2005) formulas were applied. BRB member behaves according to a bilinear force-deformation relationship with strain hardening. In Figure 102 is presented the BRB behaviour model for all three storeys.
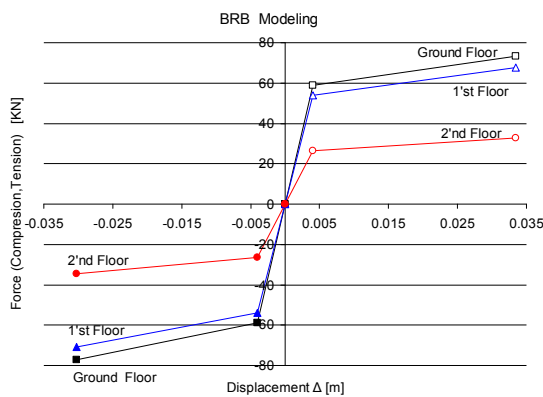


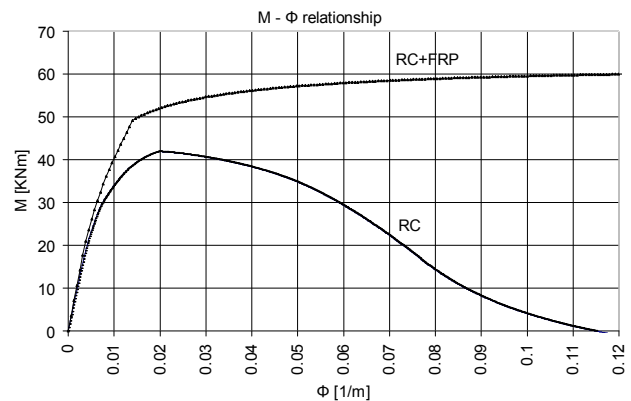Figure 102. BRB behavior model.



Figure 103. Effect of confinement by FRP on the moment-curvature relationship corresponding to an axial force of 389.6 kN from seismic load combination

In order to enhance ductility of reinforced concrete columns, their strengthening with FRP was considered. The fabric was applied in horizontal layers, its effect being confinement of concrete. The effect of confinement by FRP was determined according to FIB Bulletin 14 (2001), and consisted in an increase of concrete compression strength (from 12.5 N/mm2 to 40.8 N/mm²) and ultimate strain (from 0.005 to 0.02). A more favourable behaviour of the confined columns is resulting (Figure 103).

Pushover analysis and time history analysis were applied in order to evaluate the differences between the original frame (MRF) and the retrofitted ones. Performance of the structure was evaluated in terms of displacement demands corresponding to attainment of inelastic deformation capacities at the ultimate limit state (ULS). Development of plastic mechanism was also observed. Figure 104 to Figure 106 summarize the main results of these analyses. Details are presented in Dubina et al. (2007) and Bordea et al. (2008).

The analysis showed the inelastic demands in beams and BRB's are significant. From pushover analysis ultimate plastic deformations in bracings and beams are attained at top displacements lower than the displacement demand at the ultimate limit state. However, from time history analysis it can be seen a very good improvement of the seismic behaviour as the top displacement is reduced significantly (Table 20) and no plastic hinge in columns occurred at the ultimate limit state; the plastic hinges are initiated first in BRB, after followed by those in beams. Table 21 shows the ductility demands for BRB, as they resulted from the analysis.
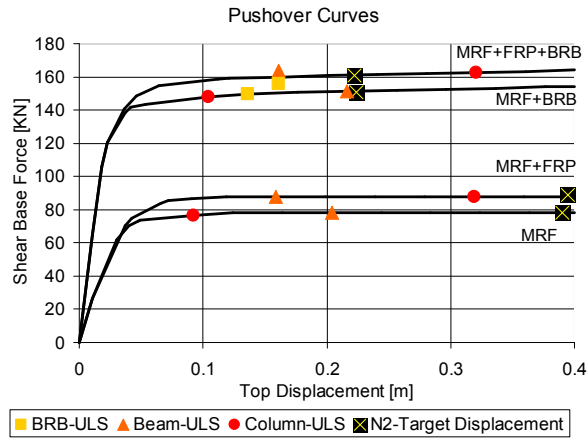
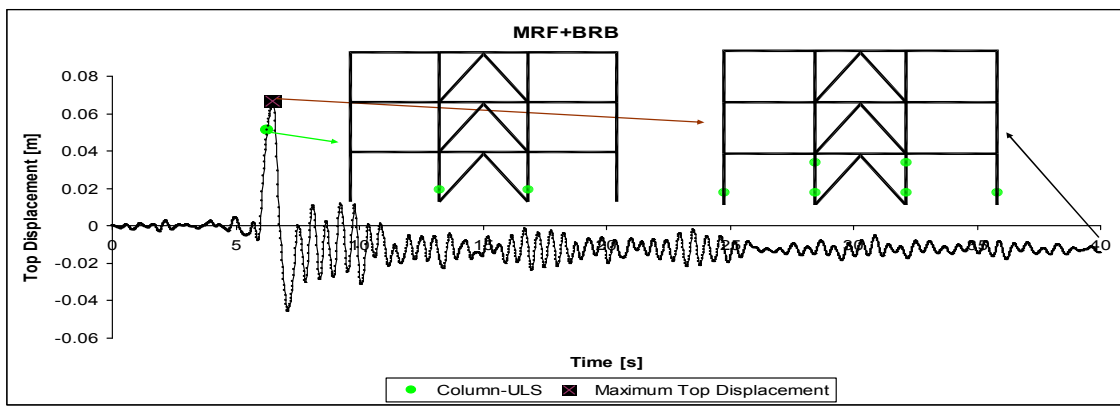Figure 104. Pushover curves of the analysed frames.



Figure 105. Top displacement time history and plastic hinges that reach ultimate rotation for RC frame strengthening with BRB.
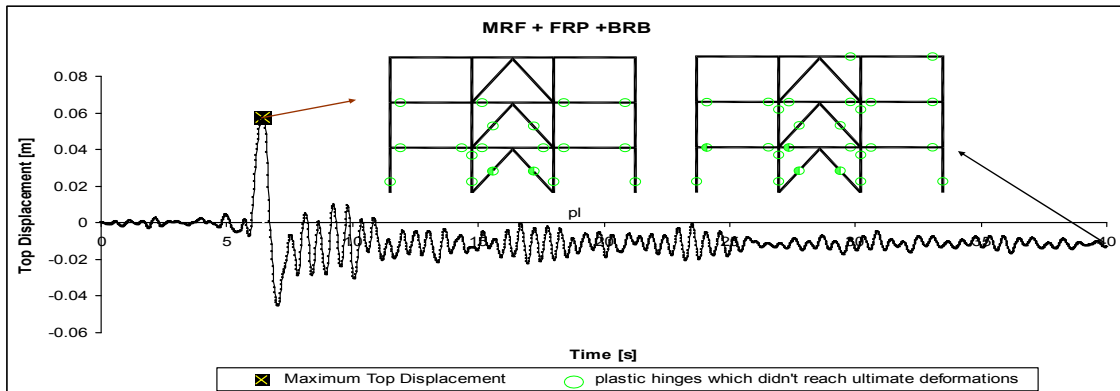


Figure 106. Top displacement time history and plastic hinges that reach ultimate rotation for RC frame strengthening with both BRB and FRP.

Table 20. Top displacement of 2D RC frame during nonlinear analysis.

| Pushover (EC8) - target displacement demand, m | | Time-history analysis - maximum top displacement, m | |
|---|---|---|---|
| (-) FRP* | (+) FRP** | (-) FRP* | (+) FRP** |
| 0.224 | 0.222 | 0.067 | 0.057 |

* (-) FRP – without FRP contribution (confinement of the columns)
** (+) FRP – with FRP contribution (confinement of the columns)

Table 21. Defromation demands and FEMA acceptability criteria for BRBs at Life Safety performance objective (mm).

|         | Pushover | Time History | FEMA 356 |
|---------|----------|--------------|----------|
| (-)FRP  | 62.0     | 24.4         | 28       |
| (+)FRP  | 56.0     | 16.6         | 28       |

The maximum displacement of the BRB elements correspond to the ultimate limit state (ULS) deformation. Pushover and time history analyses were applied according to the Romanian seismic loading (Bucharest spectrum and Vrancea accelerogram 1977 on NS direction with a peak ground acceleration of 1.949 m/s²). It could be considered as an approximation of ULS deformation with LS (life safety) from FEMA 356 (2000). In order to check the capacity of BRB members to comply with these demands an experimental program was carried out.

To design the experimental program the middle span from the ground floor of the analysed frame was isolated and considered to be pinned at the supports (see Figure 107).
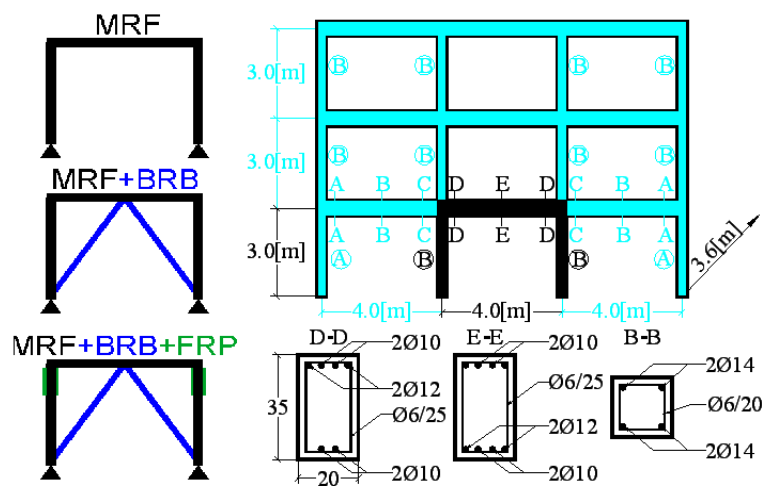


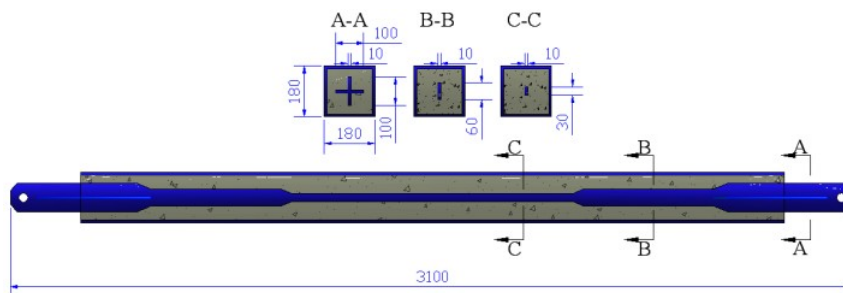Figure 107. Proposed experimental reinforced concrete frame.



Figure 108. Proposed BRB system.

The BRB design follows the general rules of EN 1998-1 for steel concentrically braced systems, and the specific rules of AISC 2005, respectively. A steel plate core is inserted in a steel tube filled with concrete represents the BRB system. The steel plate resists the loads and dissipates seismic energy by yielding while the steel tube and the concrete restrain the buckling of the core plate (Figure 108). In order to study the behaviour of BRB element, a subassembly test was prepared according to AISC 2005 specifications, as it can be seen in Figure 109. The following types of materials were used: for the core - steel S275 ($f_y$ = 275 N/mm², $f_u$ = 400 N/mm², A% = 34%); three different as unbonding materials i.e. polyethylene film, rubber, asphaltic bitumen and concrete C40/50 as infill material. Two monotonic (tension and compression) and two cyclic tests for each BRB unbonding type have been considered.
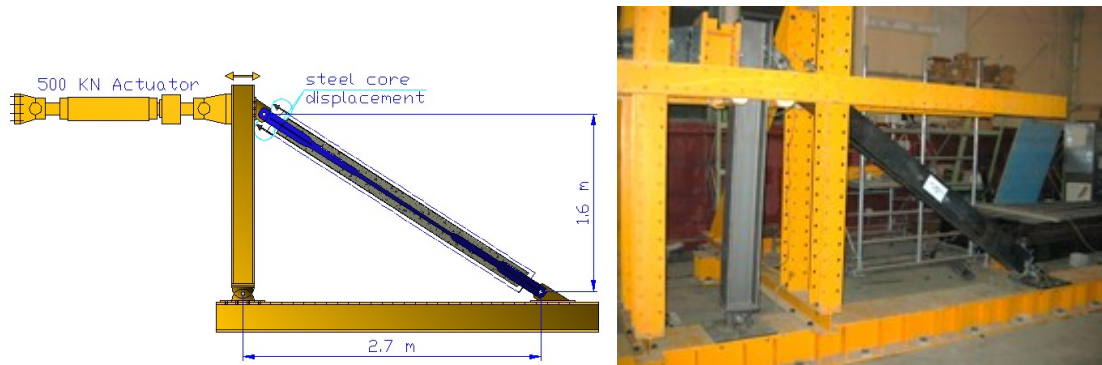
Figure 109. Testing set-up.

The following parameters have been monitored during monotonic and cyclic tests, conducted in displacement control: steel core displacement, pinned end connection displacement (to check steel plate bearing) and global rotation of the BRB. The yield displacement ($D_y$) and corresponding yield force ($F_y$) have been evaluated from monotonic tests. The results are summarized in Figure 110. The reference values of $F_y$ and $D_y$ were determined as the average of the whole results ($D_y$ = 1.91 mm and $F_y$ = 128 kN).



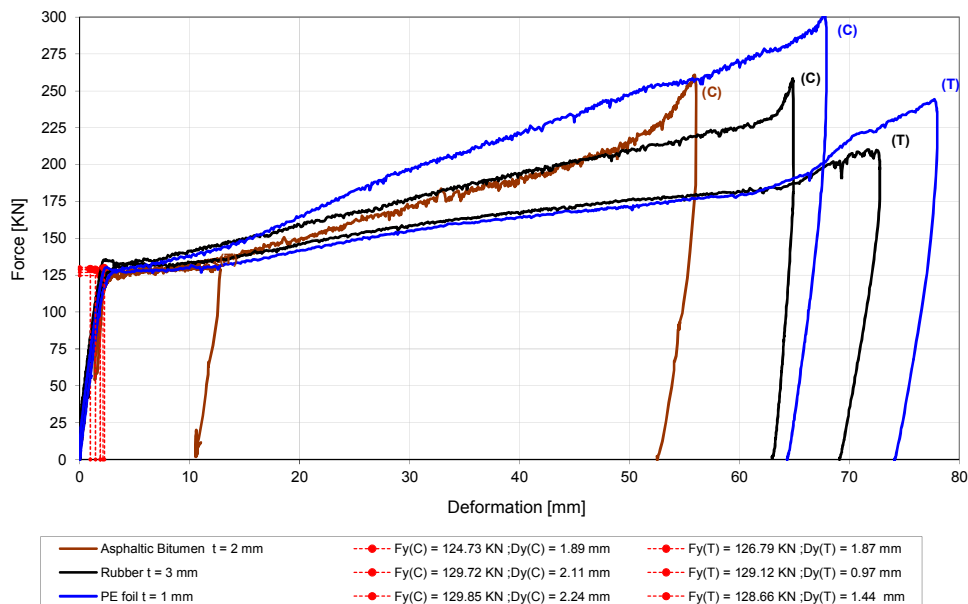| Asphaltic Bitumen  t = 2 mm | Fy(C) = 124.73 KN ;Dy(C) = 1.89 mm | Fy(T) = 126.79 KN ;Dy(T) = 1.87 mm |
| Rubber t = 3 mm | Fy(C) = 129.72 KN ;Dy(C) = 2.11 mm | Fy(T) = 129.12 KN ;Dy(T) = 0.97 mm |
| PE foil t = 1 mm | Fy(C) = 129.85 KN ;Dy(C) = 2.24 mm | Fy(T) = 128.66 KN ;Dy(T) = 1.44  mm |

Figure 110. The monotonic behaviour of the BRB tests (compression vs. tension).

Two loading protocols were applied on during cyclic tests. For the first specimen the cyclic loading was applied according to AISC (2005), characterized by a repetition of two cycles at $D_y$, followed by groups of two cycles in increments of 0.5 $D_{bm}$ – until the cumulative inelastic deformation reaches $200D_y$ at least. For the second specimen, the modified ECCS cyclic loading protocol was applied; it is characterized by a single loading at $D_y/4$; $2D_y/4$; $3D_y/4$ and $D_y$, followed by three repetitions at $4D_y$, $8D_y$ until a cumulative inelastic deformation of $200D_y$ is reached at the end of the protocol. One notice the cumulative plastic displacement of $200D_y$ was kept in both protocols in order to have a common basis of reference. The two protocols are comparatively represented in Figure 111.

It can be observed that compared to AISC, the ECCS protocol produces more fatigue effects due to an increasing number of cycles leading to a the collapse of BRB member, at smaller displacements (Table 22). The BRB of polyethylene film unbonding material appears to be the best one.
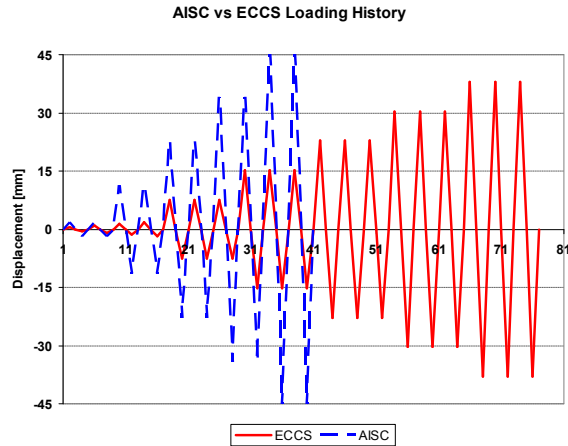
Figure 111. The AISC and ECCS loading protocols for cyclic tests.

Table 22. Summary of cyclic tests.

| Unbonding material | | $D_y$, mm | $F_y$, kN | AISC | | | | ECCS | | | |
|---|---|---|---|---|---|---|---|---|---|---|---|
| | | | | no. of cycles | $D_u(+)$, mm | $D_u(-)$, mm | $D_{cum}$, mm | no. of cycles | $D_u(+)$, mm | $D_u(-)$, mm | $D_{cum}$, mm |
| Polyethylene film | C | 1.89 | 124.7 | 10 | 45.8 | 46.1 | 448 | 16 | 30.5 | 31.4 | 432 |
| | T | 1.87 | 126.8 | | | | | | | | |
| Asphaltic Bitumen | C | 2.11 | 129.7 | 7 | 35.0 | 34.3 | 196 | 13 | 22.8 | 22.9 | 252 |
| | T | NA | NA | | | | | | | | |
| Rubber | C | 2.24 | 129.9 | 9 | 45.6 | 45.6 | 356 | 14 | 30.4 | 30.4 | 312 |
| | T | 1.44 | 128.7 | | | | | | | | |

$D_u(+)/(-)$– max/min plastic displacement
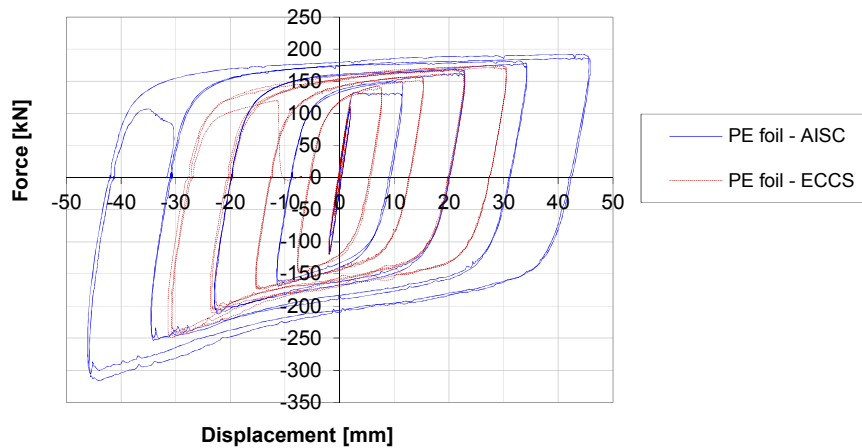
$D_{cum}$ – cumulative displacement



Figure 112. Cyclic response of BRBs with PE foil.

The cyclic behaviour in tension and compression of BRB, using polyethylene film, shown in Figure 112, proves a stable hysteresis loops, almost the same capacity in compression and tension and the same rigidity.

Figure 113 shows one of the tested specimen after test. One observes the sine plastic buckling shape which enabled for stable and highly dissipative loops during cyclic test.
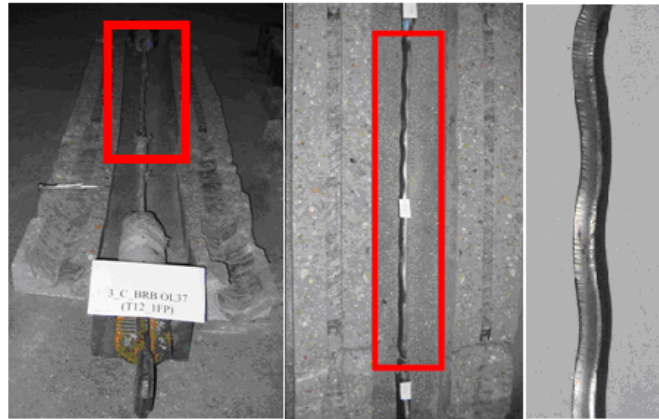
94

Figure 113. BRB uncovering and steel core deformations (local buckling).

Table 23. Ultimate deformation of BRBs under cyclic load.

| Unbonding material | AISC | ECCS |
|---|---|---|
| Polyethylene film | +/-46 | +/-31 |
| Asphaltic Bitumen | +/-34 | +/-22 |
| Rubber | +/-45 | +/-30 |

In order to compare the demanded plastic displacement capacity for BRB, resulted from analysis (see Table 21), in Table 23 were extracted the experimental values of ultimate displacements obtained during the cyclic tests. If the AISC protocol is considered, all BRB types conveniently satisfy the demand as well as the FEMA requirements. In case of asphaltic bitumen unbonding BRB, the ECCS protocol leads to a lower value than the demanded one. However, since three repetitions at maximum amplitude of seismic motion have been never recorded during historical earthquakes, one considers the AISC protocol has to be taken as reference in such a kind of tests.

The effectiveness of BRB systems used for strengthening and provide energy dissipation capacity of a poor reinforce concrete frame has been analysed. Numerical analysis showed that the use of BRB system has to be associated with local FRP confinement of columns at least (confinement of beams would be beneficial, too). BRB specimens have been designed according to the demands resulted from the analysis and according to FEMA 356 criteria. Using the same steel core, three types of BRB have been prepared, using three different unbonding materials i.e. polyethylene film, asphaltic bitumen and rubber. Both monotonic and cyclic tests have been performed. Cyclic tests have been carried out according to both AISC 2005 and ECCS Recommendations. All the three BRB solutions satisfied the demand, however the one using polyethylene film proved a better behaviour.

## 2.4.2  STRENGTHENING OF MASONRY WALLS WITH METAL-BASED TECHNIQUES

Masonry buildings are widely spread in Europe. Most of these structures represent historical constructions with symbol value for many towns or countries. Their functionality is diverse, including residential houses, hospitals, schools and other essential facilities. Therefore, these types of structures are important from many points of view: life safety, economical aspects and cultural heritage preservation. Erected in a period when design methods where poor or missing, and the knowledge regarding seismic action was almost inexistent, these buildings need a structural upgrade in order to respect safety criteria of modern codes.

Poor behaviour of masonry structures under seismic action is due to the lack of resistance, tensile stress mainly, small deformation capacity and low ductility. Moreover, under seismic action the masonry, because it is stiff and heavy, attracts significant inertial forces. Common damage patterns for masonry buildings recorded during earthquakes can be classified in the following four categories:
- Out-of-plane damage or collapse of walls;
- In-plane shear or flexural cracking of walls;
- Loss of anchorage of walls to floor or roof diaphragms;
- Damage or collapse of corners.

Out-of-plane failure modes, e.g. falling down, can be a result of: load capacity exceeded due to inertial seismic forces, excessive deflection imposed on walls from diaphragm action, lack of anchorage, poor possibility of transferring deflection and inertial forces to horizontal elements. In-plane damage can be a result of: diagonal cracking through masonry units due to excessive principal stress (tensile stress), shear sliding along bed joints, excessive toe compressive stress causing crushing (sliding shear), or tensile cracking normal to bed joints resulting in rocking (bending). The interaction of in-plane and out-of-plane forces has as consequence failure of corners.

This research focused on strengthening techniques aiming to improve the in-plane behaviour of masonry panel. However, they obviously enhance the out-of-plane resistance, too.

The objective of traditional consolidation techniques was mainly the local repair of damaged elements without a general strategy related to the global behaviour of the structure. At present, not only the impact of local strengthening on the global response of the structure has to be considered, but also the reversibility of the used techniques and compatibility between materials, the added and existing ones (e.g. the "mixed" action) have to be analysed and evaluated. The reversibility is very important because it offers the possibility to remove a solution when more advanced technology will be available. The use of "mixed material based technology" enables to optimise the performance of retrofitted structure.

For this reasons, combining metal sheeting, which is resistant and ductile, with masonry, providing a proper connecting system, seems to be a suitable solution. The use of "dry" connection enables easy removal of metallic elements. Additionally, this solution offers the advantage of high mechanical properties, e.g. strength and ductility, without changing too much the initial rigidity. This technique can provide a stable post-cracking behaviour to the masonry wall. Moreover, a performance based strengthening methodology could be developed.

Two strengthening solutions were proposed and investigated within the research program. The solutions use steel (SSP) or aluminium (ASP) sheeting plates (see Figure 114), and steel wire mesh (SWM), respectively (see Figure 116).

Connection of the metal sheets plates to the masonry wall is realised in two ways: chemical anchors (CA) and prestressed ties (PT), placed at 200-250 mm. The wire mesh is glued using epoxy resin. Both systems can be applied on one side or both sides of the panel. It is expected that the system with metallic elements on both sides to perform better, but it isn't always possible due to

architectural reasons. Such a type of solution can be successfully applied in case of masonry walls, but it is not appropriate in case of masonry vaults and arches.

Observing the behaviour of a masonry wall with openings it is easy to identify the weak regions that need strengthening with metal plates (SP) or wire mesh (WM) (see Figure 115).

The application technology is rather simple. In the case of metallic plates they must be previously drilled. Afterwards the plate is placed on the wall, anchor holes are drilled in the masonry wall through the plate holes. The dust is blown away from the holes, followed by injection of epoxy resin and fixing of chemical anchors (see Figure 116). Prestressed ties are applied similarly, but no resin is used, and the ties are tightened using a torque control wrench.
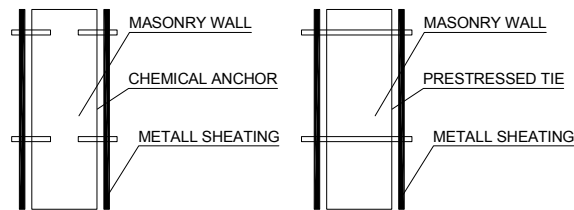
Figure 114. Proposed solution.

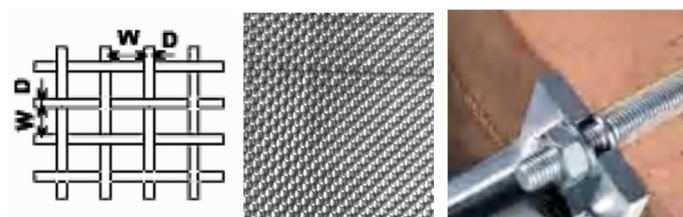Figure 115. Weak area on masonry façade and location of SP or WM.

Figure 116. Wire mesh geometry and texture and chemical anchor.

The mesh is produced either as galvanised steel or stainless steel bidirectional fabric. Spacing of the mesh is between 0.05 and 16 mm, while wire diameter is between 0.03 and 3.0 mm. Tensile strength reaches 650-700 N/mm², while elongation is about 45-55% in the case of stainless steel wires. For galvanised steel wire, tensile strength is usually in the range of 400-515 N/mm².

Application of wire mesh (see Figure 116) requires a previous preparation of the walls to obtain a smooth surface. The preparation of resin is similar to the one used for Fiber Reinforced Polymers (FRP). The resin is applied in two steps: a fluid layer is applied first, and after it is dried, a second

thick fluid layer is applied to embed the mesh. For large surfaces the mesh should be fixed to the wall with nails in order to keep plain its surface. It is important to mention that, by heating the resin layer, the wire mesh can be removed.

In order to validate the two solutions, an experimental program was carried out. It included:
- Material tests;
- Preliminary tests on 500 x 500 mm specimens;
- Full scale tests on 1500 x 1500 mm specimens, both under monotonic and cyclic loading.

Some simple numerical calculations have been performed to determine the thickness of steel shear plate in order to obtain a rational behaviour. On this purpose, three preliminary design criteria expressed in terms of stiffness, stability and strength have been used. First material tests were performed in order to establish strength and stiffness parameters. They are summarized in Table 24.

Table 24. Summary of material tests

| Masonry component | Elastic modulus of masonry |
| | Compression test on brick |
| | Compression test on mortar |
| | Tension test on mortar |
| Steel wire mesh | Tensile test on wire |
| | Tensile test on mesh |
| Connectors | Tensile test on ties |
| Tensile test on steel plates | |
| Tensile test on aluminium plates | |

First criterion is used to obtain comparable stiffness of the metallic sheeting plates with masonry panel, in order to provide a uniform distribution of stresses between wall and sheeting. To evaluate the rigidity of the wall and sheeting plate the following formulas have been used:

$$k_m = \frac{1}{\dfrac{h_{eff}^3}{E_m I_g} + \dfrac{h_{eff}}{A_v G_m}}$$

(22)

where $k_m$ = stiffness of masonry panel; $h_{eff}$ = effective wall height; $E_m$ = longitudinal elastic modulus of masonry; $I_g$ = moment of inertia; $A_v$ = shear area; and $G_m$ = transversal elastic modulus of masonry.

$$k_{plate} = \frac{1}{\dfrac{h_{eff}}{A_v G_s}}$$

(23)

where $k_{plate}$ = stiffness of steel plate; $h_{eff}$ = height of plate; $A_v$ = shear area, and $G_s$ = transversal elastic modulus of steel (Astaneh-Asl, 2001).

Considering known all material parameters and by equating the two relations, a 2.16 mm thickness demand for the steel sheeting was obtained.

Second condition follows to obtain a compact plate in order to prevent local buckling and assure dissipation of energy through plastic bearing work in connecting points only. To establish the "non-compact" behaviour domain the following criterion was used:

$$1.10\sqrt{\frac{K_vH}{F_{yw}}} \geq \frac{h}{t_w} \geq 1.37\sqrt{\frac{K_vH}{F_{yw}}} \tag{24}$$

where $K_v$ = plate buckling coefficient; $H$= horizontal load of the panel; $F_{yw}$ = yielding stress of steel; $h$ = distance between connectors (imposed by masonry texture); and $t_w$ = steel plate thickness.

From equation (24), the compactness criterion results as $t_w \geq 2.27$ (mm).

A more complex methodology, to evaluate the resistance of each component of the system, proposed by the producer of chemical anchor can be used. Three components govern the behaviour of the chemical connection, e.g. the matrix (masonry with epoxy resin), steel anchor and steel plates. It is believed that the most desirable failure mode is the bearing of the steel hole (e.g. in the connecting points). In order to obtain this failure mode, the bearing resistance should be less than the minimum between the shear resistance of connector and crushing resistance of matrix.

$$N_{bearing} \leq \min(N_{masonry}, N_{conector}) \tag{25}$$

For chemical anchors, the design methodology suggested by producer (Hilti-Catalogue, 2005) has been adapted for masonry matrix:

$$V_{Rd,c} = V_{Rd,c}^0 \cdot f_{BV} \cdot f_{\beta V} \cdot f_{AR,V} \tag{26}$$

where $V_{Rd,c}$ = matrix edge resistance; $V_{Rd,c0}$ = basic matrix edge resistance; $f_{BV}$ = matrix strength influence; $f_{\beta V}$ = load direction influence; and $f_{AR,V}$ = spacing and edge coefficient.

Two cases were considered: ø8 and ø10 connector diameter. Corresponding plate thickness amounted to 2.20 and 2.48 mm. It was decided to use a 3 mm thickness steel plate of S235 grade when applied on one side and 2 mm thickness plate of S235 grade when applied on both sides. Alternatively, 5 mm aluminium plates were used (99.5% Al 1050 H14 - $R_{p0.2}$=105 N/mm²).

Due to the inherent approximations in design assumptions and the poor accuracy of analytical approach based on available formulas, it was decided to perform a series of test on small specimens in order to validate and calibrate the proposed techniques. The tests on small specimens are summarized in Table 25.

Table 25. Tests on small specimens

| Preliminary | Masonry panel | |
|---|---|---|
| Connection | Chemical anchor (CA) | ø8 |
| | | ø10 |
| | Prestressed ties (PT) | ø10 – 0% |
| | | ø10 – 100% |
| Diagonal tension test | Steel wire mesh (SWM) | |
| | Steel shear panel (SSP) | Chemical anchor |
| | | Prestressed ties |

Some preliminary tests were carried out on unreinforced masonry panels (brick unit strength of 10 N/mm² and mortar strength of 13 N/mm²) to obtain reference values.

Connection tests were performed in order to establish the connector diameter and to assess the influence of prestress level of steel ties. The experimental set-up is presented in Figure 117.

Chemical anchors ø8 and ø10 diameters gr.5.8 have been tested. The failure mode for ø8 was the shear of connector and for ø10 the shear of connector and crushing of masonry. For the large specimen tests, a ø10 connector was chosen, due to the more efficient behaviour and resistance.
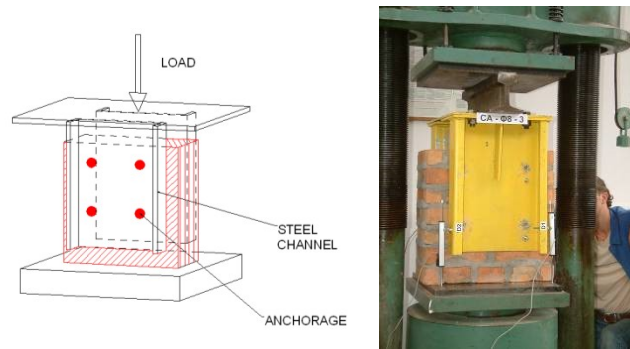
Figure 117. Experimental set-up and testing machine for connectors.

Two prestressing levels have been applied for the ø10 ties gr.5.8 (i.e. snug tightened ties (0% prestress) and full prestress (100%)). The failure mode was shear of ties, masonry specimens remaining almost intact. It was noted that the prestress level increases the resistance of connection due to confinement of masonry. In comparison with chemical anchors, prestressed ties led to more resistant and more rigid specimens.

System tests were carried out in order to validate the analytical assumption in case of shear plates and to choose a proper steel wire mesh. The experimental set-up on small specimens and a sample test on unreinforced masonry panel are presented in the Figure 118.
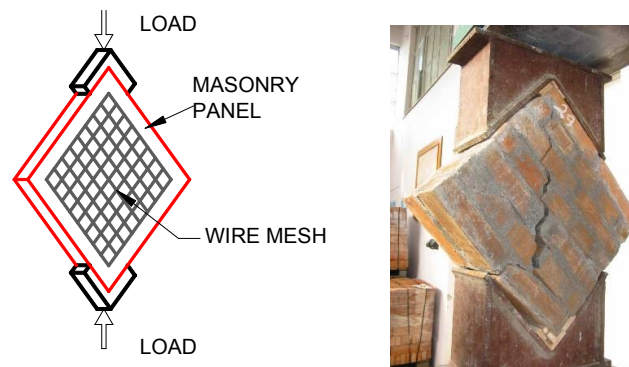


Figure 118. Experimental set-up for split test.

Steel shear plates S235 grade of 2 mm thickness on both sides and 3 mm thickness on one side, connected with chemical anchors and prestressed ties were tested.

There are no analytical procedures to design the steel wire mesh reinforced masonry, therefore calibration was based on experimental test. The purpose of tests was to select the appropriate resin and wire mesh to be applied on large specimens. In the first step six types of wire mesh were tested.

Compared to FRP technique a thicker fluid resin was selected. In order not to change too many parameters and based on the experimental results, the following wire meshes were chosen: zinc coated (ZC) 0.4x1.0 (D x W), stainless steel (SS) 0.4x0.5 and 0.4x1.0. The failure modes are shown in Figure 119:
- WM3 – sudden wire mesh rupture simultaneous with masonry crack – strength improvement (weak WM);
- WM5 – debonding of wire mesh, rupture in resin – strength improvement, energy dissipation due to the successive debonding (strong WM);
- WM6 – wire mesh yield – improvement of resistance and ductility (optimal).
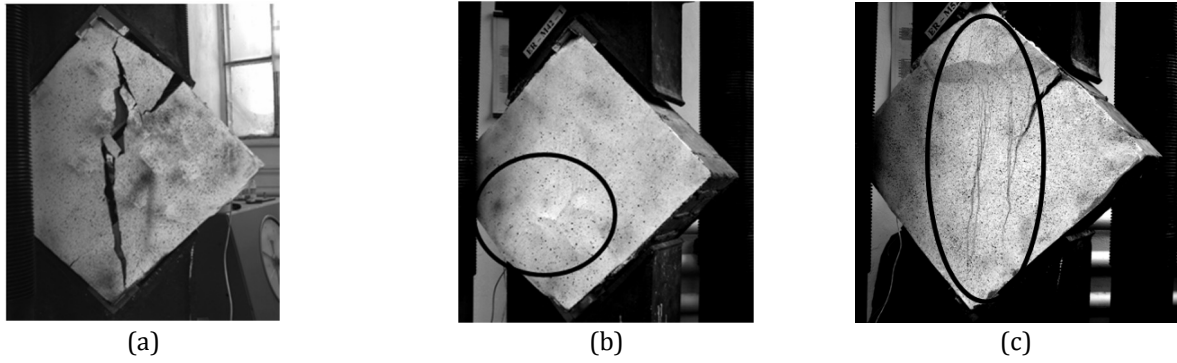
Figure 119. Failure mode for SMW on both sides a) ZC 0.4x1.0 b) SS 0.4x0.5 and c) SS 0.4x1.0.

Table 26. Tests on large specimens.

| | | | |
|---|---|---|---|
| Monotonic | Reference masonry wall test | | REF |
| | Steel shear panel | Chemical anchor | SSP-CA |
| | | Prestressed ties | SSP-PT |
| | Aluminum shear panel | Chemical anchor | ASP-CA |
| | | Prestressed ties | ASP-PT |
| | Steel wire mesh | | SWM |
| Cyclic | Reference masonry wall test | | REF-c |
| | Steel shear panel | Chemical anchor | SSP-CA-c |
| | | Prestressed ties | SSP-PT-c |
| | Aluminum shear panel | Chemical anchor | ASP-CA-c |
| | | Prestressed ties | ASP-PT-c |
| | Steel wire mesh | | SWM-c |

Based on these observations, the stainless steel wire mesh 0.4x1.0 was chosen to be applied on large specimens.

The experimental program on large specimens is summarised in Table 26. The tests were carried out in two different experimental frames, one for monotonic loading and one for cyclic loading. The tests set-up is presented in Figure 120.

Loading was applied using displacement control, with lateral drift of the panel being used as control parameter. In case of cyclic loading the following loading protocol was used: one cycle at ±0.5 mm, ±1.0 mm, ±1.5 mm, ±2.0 mm, ±3.0 mm, ±5.0 mm, ±7.0 mm, ±9.00 mm, ±11.00 mm, etc. The "yield" displacement, $e_y$, was considered when significant stiffness degradation was observed. After "yielding", three cycles at $e_y$, $1.5e_y$, $2e_y$, etc. were applied, until the failure of specimen occurred.
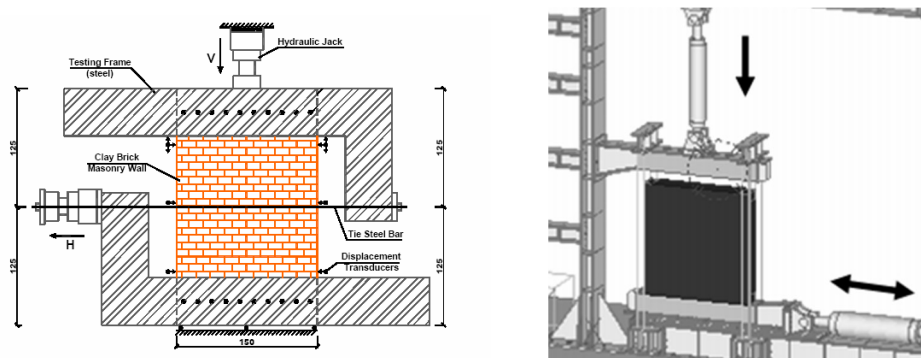


Figure 120. Testing frames for monotonic/cyclic loading.

Diagonal failure mode was observed for all specimens, both under monotonic and cyclic loading. Due to flexibility of testing frame used for cyclic loading, a more substantial damage at the corners of panel was observed in comparison with monotonic tests. However, for cyclic loaded specimens the characteristic failure was also the diagonal shear, but with a small influence due to eccentric compression. A significant improvement in terms of ultimate displacement (that shows significant improvement in ductility), and also the increase in strength, with a slight increase in stiffness were recorded for all specimens. An overview of qualitative performance in terms of strength and ductility of tested specimens, related to unreinforced masonry, is presented in Table 27.

Table 27. Large specimens' qualitative results

| Specimen | Monotonic | | Cyclic | |
|---|---|---|---|---|
| | Resistance | Ductility | Resistance | Ductility |
| ASP–CA-1 | → | ↗ | ↗ | ↗ |
| ASP–CA-2 | ↑ | ↑ | ↗ | ↗ |
| ASP-PT-1 | ↗ | ↗ | ↗ | ↗ |
| ASP-PT-2 | ↑ | ↑ | ↑ | ↑ |
| SSP–CA-1 | → | ↗ | → | ↗ |
| SSP–CA-2 | → | → | → | ↗ |
| SSP-PT-1 | ↗ | ↗ | → | ↗ |
| SSP-PT-2 | ↗ | ↑ | ↗ | ↗ |
| SWM-1 | → | → | ↗ | → |
| SWM-2 | ↑ | ↗ | ↑ | ↗ |

Legend → slight        ↗ moderate      ↑ large increase
1- one side;      2- both sides

For the one side sheeting under cyclic loading a significant out of plane deformation was observed. The force - displacement relationships are presented for ASP-PT-2, monotonic and cyclic specimens (see Figure 122 and Figure 124), as well as their failure modes (see Figure 121 and Figure 123).



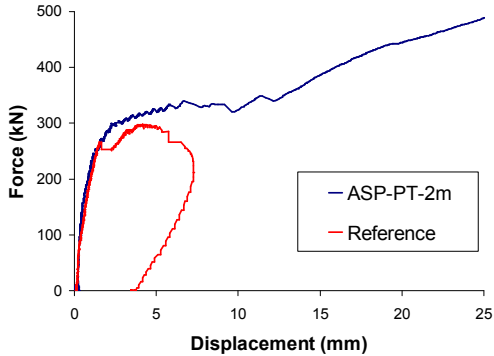Figure 121. Failure mode for ASP-PT-2m



Figure 122. Monotonic test on aluminium shear panel

Due to large in-plane stiffness of masonry walls, the strengthening solution does not avoid completely damage to masonry. A limited amount of damage to masonry has to be allowed in order to take benefit from ductility of the metal used for sheeting. Aluminium is believed to be particularly suitable in this case, due to a more favourable strength-to-stiffness ratio than steel.

It can be observed that, despite strengthening, the masonry panel cracks at almost the same force and displacement as reference panel. The mixed masonry-metallic plate system is activated only

after masonry cracking. This can be observed also by the fact that the initial stiffness of both strengthened and reference panels does not change. This is an advantage for global behaviour of retrofitted building.

The monotonic curves (see Figure 122) show an important increase in terms of resistance, but the main advantage of this system seems to be the very large ultimate displacement that assures a very stable post-cracking behaviour and a large ductility. Also, for cyclic loading this system has proved his validity by increasing the resistance and obtaining a good hysteretic behaviour despite of significant pinching (see Figure 124).



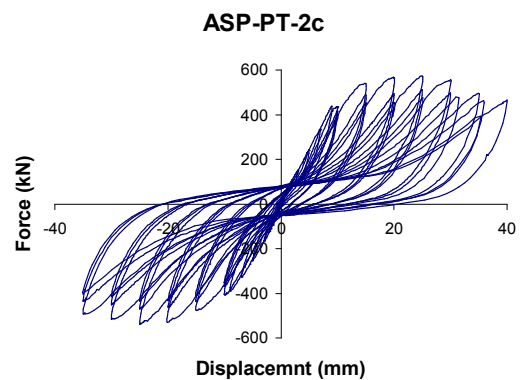Figure 123. Failure mode for ASP-PT-2C



Figure 124. Cyclic test on aluminium shear panel connected with prestressed ties

The proposed strengthening solutions are an alternative to FRP technology enabling to obtain a ductile increase of strength, but without increasing the stiffness of the wall. It can be concluded that steel plates increases mainly the ductility, while wire mesh increases the resistance. Both techniques are more efficient when applied on both sides. The prestressed tie connections seem to be more appropriate and the specimens sheeted with aluminium plates have shown a better behaviour than ones sheeted with steel.

## 2.4.3   PUBLICATIONS

[1]   T. Arangelovski, G. Altay Askar, F. Aras, C. Arion, D. Beg, A. Birouk, A. Bozer, G. Brando, L. Calado, M. Cherraj, B. Chesca, F. Colanzi, D. Cotofana, C. Daescu, D. Dan, M. Eleni Dasiou, M. D'Aniello, G. Della Corte, G. De Matteis, J-F. Demonceau, D. Diaconu, A. Dogariu, D. Dubina, A. El Hammoumi, A. El Mouraouah, V. Esposito, B. Faggiano, L. Fiorino, A. Formisano, K. Gramatikov, R. Gonçalves, M. Rosaria Grippa, K. Gueraoui, A. Iben Brahim, M. Jovanovski, J. Josifovski, J-P. Jaspart, M. Kasmi, M. Kerroum, S. Kourkoulis, P. Kozlevcar, L. Krstevska, R. Landolfo, E. Loznica, K. Marinelli, A. Marzo, F.M. Mazzolani, H. P. Mouzakis, T. Nagy-György, A. S. Panao, S. Panico, S-A. Papanicolopulos, K. Papantonopoulos, M. Pavel, L. Pavlovcic, V. Popa, F. Portioli, J. M. Proença, I. N. Psycharis, F. Sinur, P. Skuber, V. Stoian, A. Stratan, L. Tashkov, El Arbi Toto, R. Vacareanu, I. Vayas (2012). "Seismic Protection of historical buildings: experimental activity (FP6 PROHITECH project: Volume 3)", Federico M. Mazzolani (coordinator), Polimetrica Publisher, Italy, ISBN 978-8876991738, 780 pag.

[2]   Altay Askar, Gülay; Arion, Cristian; Barrecchia, Enrico; Beg, Darko; Bordea, Sorin; Bozer, Ali; Brando, Giuseppe; Calado, Luis; Daescu, Cosmin; Dan, Daniel; D'Aniello, Mario; Della Corte, Gaetano; De Matteis, Gianfranco; Demonceau, Jean-François; Dogaru, Adrian; Dubina, Dan; Fiorino, Luigi; Florut, Codrut; Formisano, Antonio; Gioncu, Victor; Nagy-Gyorgy, Tamas; Jaspart, Jean-Pierre; Kourkoulis, Stavros; Landolfo, Raffaele; Ly, Lam; Lungu, Dan; Mandara,

Alberto; Marinelli, Aikaterini; Mazzolani, Federico Massimo; Mosoarca, Marius; Panao, Ana Sofia; Panico, Simeone; Papanicolopulos, Stefanos-Aldo; Pavlovcic, Luka; Portioli, Francesco; Proença, Jorge Miguel; Ramundo, Felicita; Spina, Gerardo; Stoian, Valeriu; Stratan, Aurel; Thanopoulos, Pavlos; Vayas, Ioannis (2012). "Seismic protection of historical buildings: calculation models (FP6 PROHITECH project: Volume 5)", Federico M. Mazzolani (coordinator), Polimetrica Publisher, Italy, ISBN 978-8876991776, 308 pag.

[3]   Dubina, D., Bordea, S., Stratan A. (2008). "Seismic upgrading of reinforced concrete moment-resisting frame with dissipative buckling restrained steel braces". Acta Technica Napocensis. Section: Civil Engineering – Architecture. Nr. 51, vol. 1, 2008, ISSN 1221-5848, p. 353-360. Proceedings of the International Conference – CONSTRUCTIONS 2008, 9-10 May 2008, Cluj-Napoca.

[4]   Dubina, D., Bordea, S., Stratan, A. (2009). "Performance Based Evaluation of a RC Frame strengthened with BRB Steel Braces". Proc. of the International Conference on Protection of Historical Buildings PROHITECH 09, Rome, Italy, 21-24 June 2009. Ed. F.M. Mazzolani. CRC Press, ISBN 978-0-415-55803-7, p. 1741-1746.

[5]   Dubina, D., Dogariu, A., Stratan, A., Stoian, V., Nagy-Gyorgy, T., Dan, D. and Daescu, C. (2007). "Masonry walls strengthening with innovative metal based techniques". Proc. of the 3rd Intl. Conf. on Steel and Composite Structures (ICSCS07), Manchester, UK, 30 July - 1 August 2007, Eds. Wang and Choi. Taylor&Francis, ISBN: 978-0-415-45141-3, pp. 1071-1077.

[6]   Dubina, D., Stratan, A., and Bordea, S. (2007). "Seismic retrofit of r.c. frames with hysteretic bracing systems". Proc. of the 3rd Intl. Conf. on Steel and Composite Structures (ICSCS07), Manchester, UK, 30 July - 1 August 2007, Eds. Wang and Choi. Taylor&Francis, ISBN: 978-0-415-45141-3, pp. 833-839.

[7]   Bordea, S., Stratan, A., Dogariu, A. and Dubina, D. (2007). "Seismic upgrade of non-seismic r.c. frames using dissipative braces". Proceedings of Workshop in Prague 30-31/3/2007 "Urban habitat constructions under catastrophic events". COST Action C26. Ed. Wald, F., Mazzolani, F., Byfield, M., Dubina, D., Faber, M., ISBN 978-80-01-03583-2, pp.211-220.

[8]   Grecea, D., Bordea, S., Stratan, A., Dogariu, A., Dubina, D. (2008) "Soluţii moderne pentru consolidarea şi reabilitarea clădirilor amplasate în zone seismice". Structuri metalice amplasate în zone seismice - preocupări actuale. Ed. D. Dubina, V. Ungureanu. Editura Orizonturi Universitare, Timişoara. ISBN 978-973-638-377-9, p. 141-156.

[9]   Bordea, S., Stratan, A., Dubina, D. (2008). "Performance based evaluation of a non-seismic RC frame strengthened with buckling restrained braces", Proceedings of the International Symposium "Urban Habitat Constructions under Catastrophic Events", Malta, 22-23 October 2008, COST Action C26, Editors: Mazzolani, Mistakidis, Borg, Byfield, De Matteis, Dubina, Indirli, Mandara, Muzeau, Wald, Wang, p. 241-246. ISBN 978-99909-44-42-6

[10]  Dogariu, A., Stratan, A., Dubina, D., Nagy-Gyorgy, T., Daescu, C. and Stoian, V. (2007). "Strengthening of masonry walls by innovative metal based techniques". Proceedings of Workshop in Prague 30-31/3/2007 "Urban habitat constructions under catastrophic events". COST Action C26. Ed. Wald, F., Mazzolani, F., Byfield, M., Dubina, D., Faber, M., ISBN 978-80-01-03583-2, pp.201-210.

[11]  Dubina, D., Dogariu, A., Stratan, A. (2005). "Dissipative steel bracing systems for strengthening of existing reinforced concrete frames". A 3-a conferinţă naţională de inginerie seismică. Bucureşti, 9 decembrie 2005, Volumul II. pp. 183-196.

Circular hollow section braces with "true pin" connections were adopted in the design of a 29 storey building located in Bucharest, Romania. The brace uses connections with gusset plates and pin. One of the brace connections has an eccentric pin, allowing for variation of the pin-to-pin length, which facilitates erection on one hand, and allows compensation for axial forces in braces due to gravity loads on the other hand. High strength steel was used for gussets and pin, in order to keep connection dimensions to a minimum. Finite element analyses and cyclic experimental tests were performed in order to validate the seismic performance of the brace and its connection. Four tests were performed on a scaled model of the brace, for two different pin-to-pin lengths.

In-plan dimensions of a typical floor of the building are 52.0x25.6 m, while the total height amounts to 117.6 m. The structure uses steel framing for resisting gravity forces. In the transversal direction the main lateral force resisting system is composed of two reinforced concrete cores, while in the longitudinal one the cores are supplemented by steel braces located in the facade of the building. The braces are placed in X configuration developed over two storeys. This reduces the number of brace connections and helps in complying with code limitations on slenderness. Braces are realised from hot-finished Circular Hollow Sections (CHS) and have connections with pins. The structure was designed according to EN 1993-1-1 (2005) and P100-1 (2006) – the Romanian seismic design code, which is very similar to EN 1998-1 (2004). The connections were designed according to EN 1993-1-8 (2005).

There are two brace configurations: developed over two storeys, of 9300 mm pin to pin length (see Figure 125a), and developed over one storey, with an additional connection at the beam from the intermediate storey, of 4200 mm pin to pin length (see Figure 125b). The initial design used the following cross-sections: D244.5x25, D244.5x20, D219.1x20, D219.1x16 and D219.1x10, all in S355 steel. One of the pins of each of the brace features an eccentricity of 5 mm, allowing a +/- 5 mm adjustment of the pin to pin length of the brace. This allows for more relaxed erection tolerances on one hand, and reduces gravity-induced axial forces in the brace on the other hand, as the eccentric pin is mounted after casting of reinforced concrete floors.



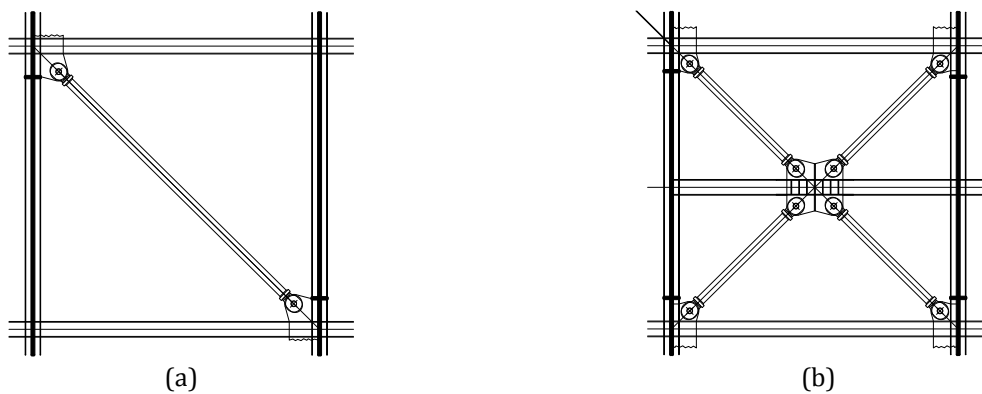(a)                                                          (b)

Figure 125. Brace configurations in the analysed structure: developed over two storeys (a) and one storey (b).

In order to have a validation of the seismic performance of the braces, a series of numerical simulations and experimental tests were performed, which are described in the following sections.

The non-dimensional slenderness $\bar{\lambda}$ of braces used in the structure varied between 1.53 and 1.72 for long braces (9300 mm), and between 0.69 and 0.78 for short braces (4200 mm). The buckling length as considered to be the distance between the pins. All braces were of class 1 according to EN 1993-1-1 (2005). Due to constraints imposed by the size of the testing platform and actuator stroke

and capacity, reduced scale experimental models were adopted. The experimental specimens were chosen so as to reproduce the non-dimensional slenderness and cross-section class of braces used in the designed structure. As a result, a class 1 cross section of 139.7x6.3 was adopted, with the pin to pin brace length of 5900 mm and 2700 mm, having $\overline{\lambda}$ values of 1.64 and 0.75 respectively. The same steel grade as in the braces from the structure was used – S355J0H.

### 2.5.1   PRE-TEST FINITE ELEMENT ANALYSES

Pre-test finite element analyses were performed with the general purpose finite element code Abaqus. Firstly a connection model was analysed, followed by a complete model of the brace assembly.

The connection of the 219.1x10 brace size was used for a detailed analysis. It consists of a central gusset connected through a pin to two external gussets, which are welded to the end plate using full-penetration welds. The initial connection design used S690Q grade steel for the pin, and S460N grade steel for the end plate and gussets. A tolerance of 1 mm on diameter was used between the pin and the gussets. Due to bearing resistance requirements, the central gusset resulted quite thick (68 mm). In order to reduce the weight of the structural steelwork and avoid disproportionate thicknesses at the welded connection between the central gusset and the beam/column, the central gusset was locally reinforced with two welded plates (see Figure 126a). An alternative solution aiming at reducing both the thickness and the workmanship was also analysed, by adopting S690Q grade steel for the gussets. In this way, the central gusset could be realised using a single piece, without reinforcements (see Figure 126b).



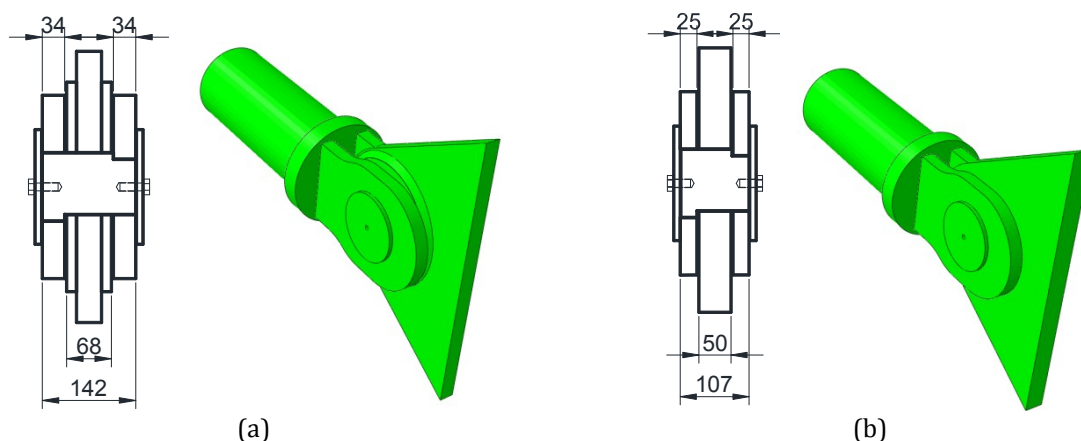(a)                                                                                           (b)

Figure 126. Connection geometry: initial design (a) and modified one (b).

The numerical model of the connection consisted of the central gusset, pin, washers, external gussets, end plate and a short portion of the CHS brace. It was discretized using three-dimensional continuum linear hexahedral elements with reduced integration and hourglass control – type C3D8R. Normal and tangential (with a coefficient of friction of 0.3) behaviour was defined at all surfaces in contact. Stress-strain relationships based on nominal material characteristics were used for all components, with the exception of the brace, for which an overstrength $\gamma_{ov}=1.25$ was applied to the yield strength. The model was subjected to tensile force equal to the design force according to EN 1998-1 (2004): plastic resistance of the brace amplified by overstrength and strain hardening ($1.1 \cdot \gamma_{ov}\ N_{pl,Rd}$). The explicit solution method was used in all cases.

Three models were analysed: the initial one (S460N gussets and reinforced central gusset), with eccentric pin (model 219x10-ecc) and constant pin (219x10-ct), and the modified one (S690Q gussets and unreinforced central gusset) with constant pin (model 219x10-ct-690) – see Figure 127.
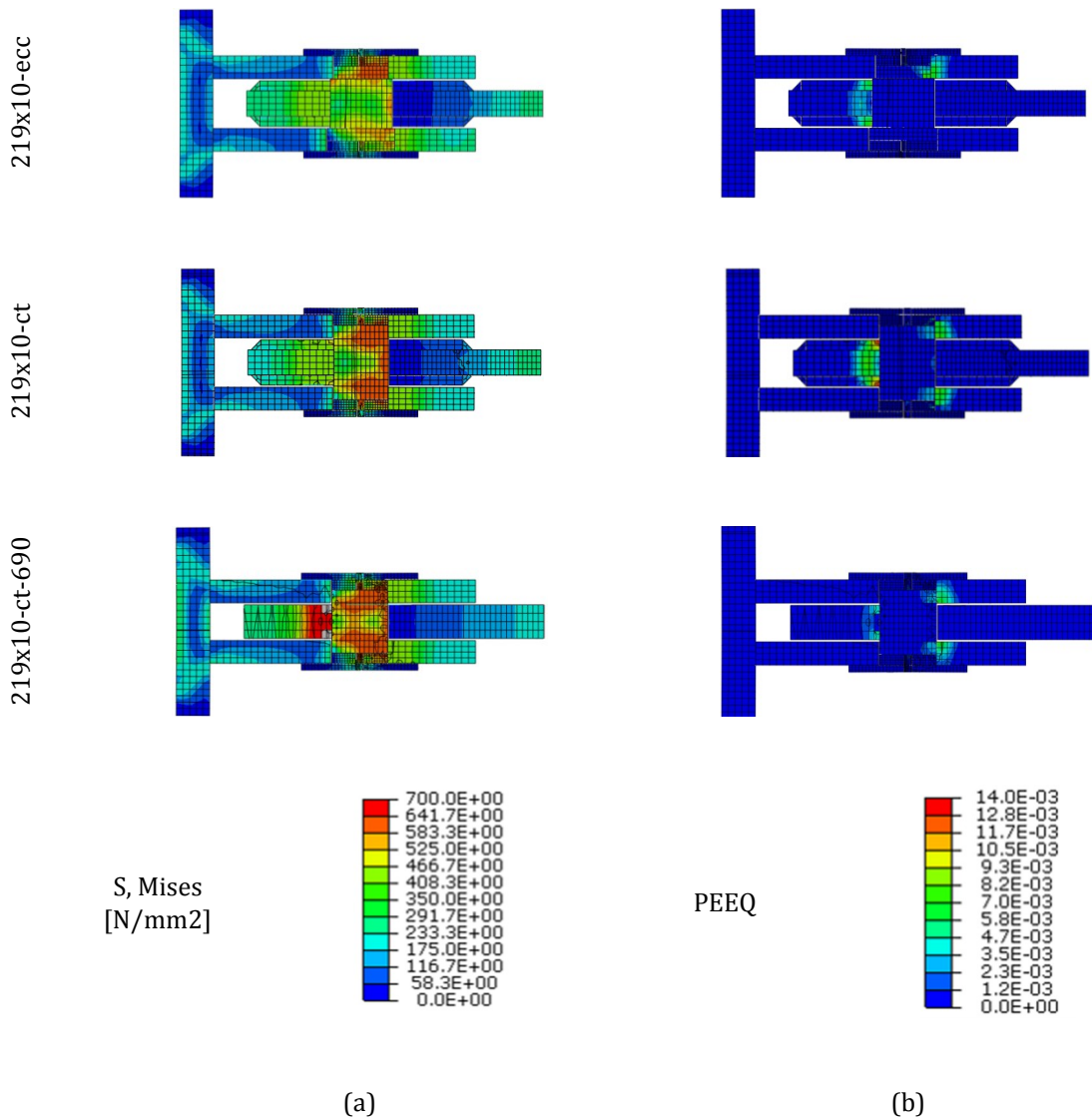
Figure 127. Distribution of von Mises stresses (a) and equivalent plastic strains (b).

Table 28. Maximum values of von Mises stresses and equivalent plastic stains in connection models.

| Model | Pin | | External gusset | | Central gusset and reinforcements | |
|---|---|---|---|---|---|---|
| | $\sigma_{VM}$ [N/mm²] | $\varepsilon_p$ | $\sigma_{VM}$ [N/mm²] | $\varepsilon_p$ | $\sigma_{VM}$ [N/mm²] | $\varepsilon_p$ |
| 219x10-ecc | 646.4 | 0.00527 | 464.0 | 0.00720 | 465.2 | 0.00938 |
| 219x10-ct | 639.5 | 0.00399 | 464.7 | 0.00800 | 471.2 | 0.01402 |
| 219x10-ct-690 | 638.9 | 0.00304 | 464.6 | 0.00772 | 706.2 | 0.00430 |

Minor plastic strains were observed in the pin and in the gusset plates of all models (see Figure 127 and Table 28). However plastic strains are local only, as they do not extend over the full cross-section. Thus, there is always a large portion of the pin or gusset that stays in the elastic range, providing the necessary strength of the connection. This behaviour is in agreement with the design followed, as the pin was designed as non-replaceable according to EN 1993-1-8 (2005).

The initial model with eccentric pin (219x10-ecc) showed slightly larger plastic strains in the pin, close ones in the external gussets and smaller ones in the central gusset and reinforcements, in

comparison with the corresponding model with constant pin (219x10-ct). On the other hand, the model that used a single-thickness central gusset and higher strength steel in gussets (219x10-ct-690) showed slightly smaller plastic strains in the pin and in the external gussets, and considerably smaller ones in the central gusset, in comparison with the initial design (219x10-ct). This is attributed to the beneficial effect of reduced bending in the shorter pin of the modified model (219x10-ct-690). Considering the above observations, the modified model using S690Q gussets was adopted for the brace.

Full-size numerical models of the experimental specimens were analysed as well. Each brace assembly consisted of a connection with constant pin, the CHS brace and a connection with eccentric pin. The same parameters as in the connection modelling were adopted, with the exception of the brace, which was meshed using shell linear quadrilateral elements with reduced integration and hourglass control of type S4R. Considering the fact that behaviour in tension is not much different than the on observed on connection model, in the following the behaviour in compression is described. Residual stresses in the brace member were ignored, as they are very low in hot-finished tubes (Ziemian, 2010). An initial imperfection of the member equal to 1/500 of the pin to pin length (the maximum delivery tolerance allowed per EN 10210-2, 2006) was considered, in the form of a circular arc. During preliminary numerical simulations, it became clear that the brace assembly is susceptible to out-of-plane buckling (out of plane of the connection). In this particular case out of plane deformations are detrimental mainly due to two reasons: (1) the rotation in the connections is perpendicular to the intended one, leading to stress concentrations and possible failure not accounted for in its design, and (2) large out of plane deformations of the brace would damage non-structural components (building facade). In order to account for the worst situation, member imperfection was oriented predominantly out-of-plane (7.5° with respect to the direction perpendicular to the plane of the gussets).

Several models of brace assemblies were subjected to compression in displacement control, up to a displacement of 30 mm, well into the post-buckling range. Figure 128a shows the deformed shape at the maximum displacement of the brace assembly with a pin to pin distance of 2700 mm, with nominal geometry and initial imperfections as described above (SP27N-C model). Lateral deformations follow the initial member imperfection and are predominantly out of plane. In an effort to understand the causes of this behaviour, two other models were derived from the reference one: with lateral deformations forced in plane (SP27N-CI) and out of plane (SP27N-CO), through some rigid frictionless surfaces. As can be seen from Figure 128b, the buckling strength of the SP27N-CI model is larger than of the SP27N-CO, the response of the reference model (SP27N-C) being basically identical to the one of the latter.

The reason for out of plane buckling of the brace, apart from the quite unfavourable orientation of the initial imperfections, is the connection itself and the circular shape of the cross-section. The in-plane connection rotation is not totally free due to friction between its components (pin and gussets). On the other hand, out of plane behaviour of the connection is very close to a perfect pin at small rotations, due to the clearance between the pin and the holes in the gussets (1 mm on diameter), as well as between the central and lateral gussets (1.5 mm). In the conditions described above, at initial stages of loading lateral deformations develop mainly in the direction of initial imperfections (out of plane). Once the wedging of the gussets and the pin occurs, out of plane rotation of the connection is not free any more, though its in-plane rotations is also restrained to some extent due to additional friction between the gussets and the pin. With reference to the SP27N-C series of models (see Figure 128b), even if the post-buckling strength of the SP27N-CI model is smaller than the one of the SP27N-CO one, "switching" to in-plane buckling at large deformations is restrained by the friction developed between the gussets and the pin, as a result of out of plane rotations of the connection.
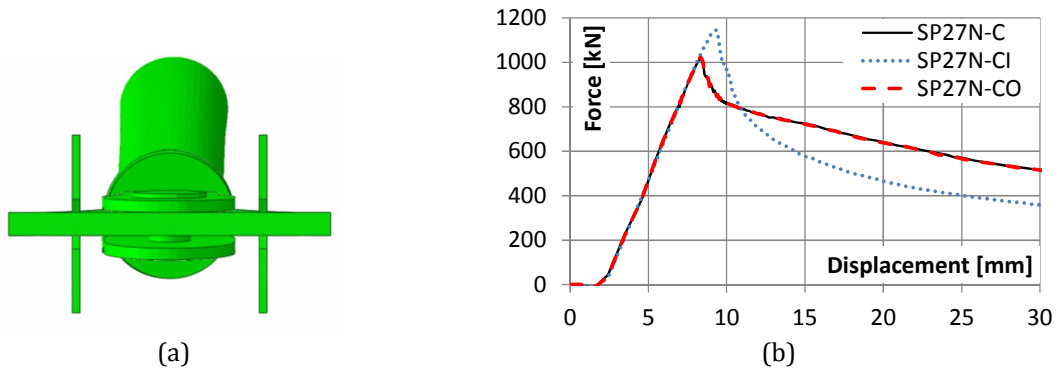
Figure 128. Deformed shape of the SP27N-C model at the maximum displacement (a) and the force-displacement relationship for SP27N-C series of models (b).
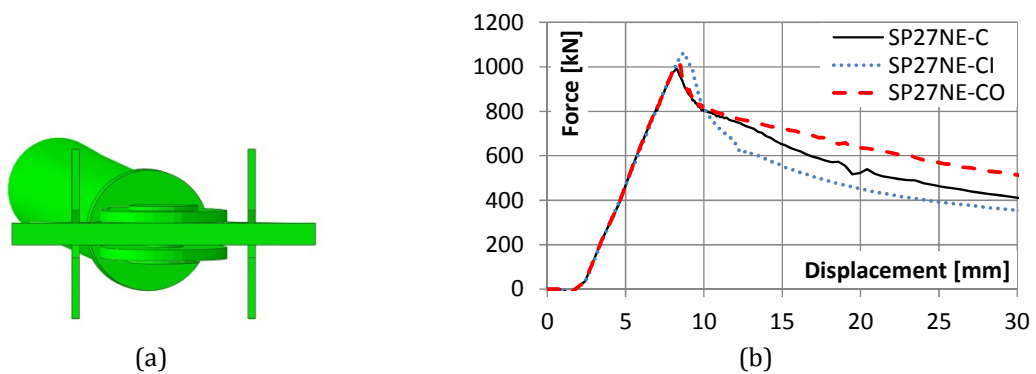


Figure 129. Deformed shape of the SP27NE-C model at the maximum displacement (a) and the force-displacement relationship for SP27NE-C series of models (b).

A possible solution was sought in the form of a design initial connection eccentricity specified in the plane of the connection (SP27NE-C series of models, see Figure 132a). The magnitude of the eccentricity (4 mm) was chosen close to the maximum initial bow imperfection of the member (L/500 = 5.4 mm). As can be seen in Figure 129a, the behaviour of the brace improved somehow, lateral deformations of the brace in the post-buckling range being predominantly in the plane of the connection, though with important component in the out of plane direction. The in-plane buckling strength (model SP27NE-CI, see Figure 129b) is now only slightly higher than the out of plane one (model SP27NE-CO). Though the reference model (SP27NE-C) buckles initially out of plane, in the post-buckling range lateral deformations develop predominantly in-plane.

A further improvement of the response of the assembly was obtained by welding two 14x14 squares along the tube perpendicular to the plane of the connection (see Figure 130a). It increases the out of plane stiffness of the tube, decreasing the out of plane lateral deformation of the brace in favour of the in-plane ones. The buckling strength of the model with lateral deformations forced in plane (SP27NES-CI) is now very close to the one of the model with lateral deformations forced out of plane (SP27NES-CO), see Figure 130b. Furthermore, the post-buckling strength of the reference model (SP27NES-C) is now very close to the one of SP27NES-CI. Additionally, this in following model used strengthened washers securing the pin (see Figure 132b).

The model of the longer brace (5900 pin to pin length) used the same connection eccentricity (4 mm), but no longitudinal stiffeners. In the post-buckling range lateral deformations are predominantly in the plane of the connection (see Figure 131a), though the in-plane buckling strength is slightly larger than the out of plane one (see Figure 131b). The SP59NE-C model initially develops mainly out of plane lateral deformations, but, at about 12 mm axial deformation, when the

in-plane moment imposed on the connection becomes larger than the resisting one due to friction, a sudden switching to in-plane buckling takes place, which becomes the governing post-buckling behaviour.
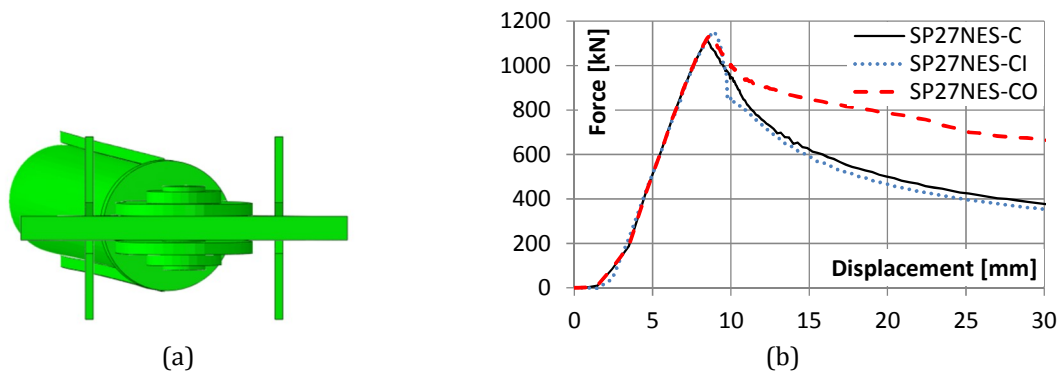


Figure 130. Deformed shape of the SP27NES-C model at the maximum displacement (a) and the force-displacement relationship for SP27NES-C series of models (b).
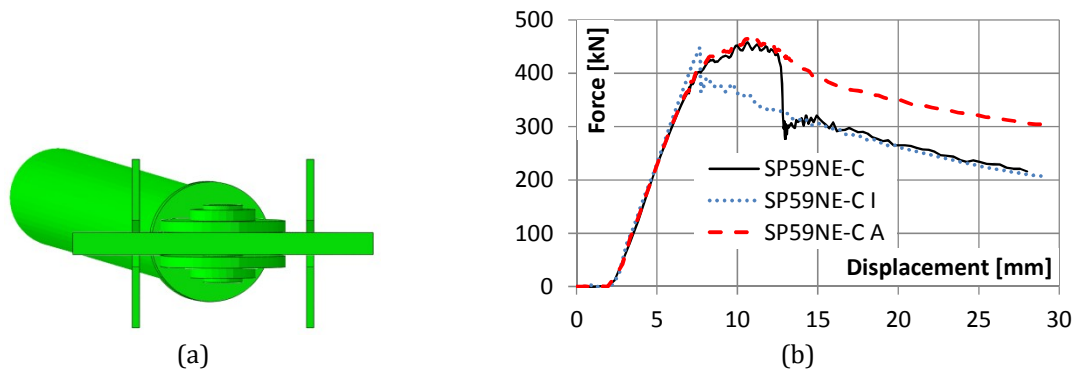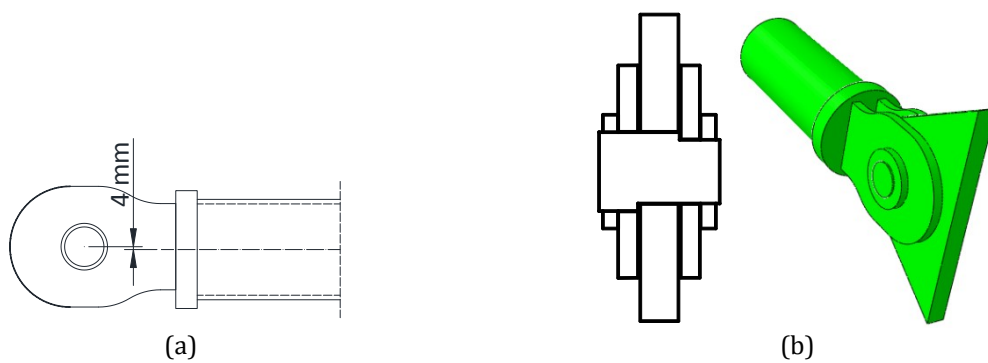


Figure 131. Deformed shape of the SP59NE-C model at the maximum displacement (a) and the force-displacement relationship for SP59NE-C series of models (b).s



Figure 132. Connection eccentricity (a) and improved connection detailing (b).

## 2.5.2   EXPERIMENTAL INVESTIGATION

The experimental program included 4 braces subjected to cyclic loading, overviewed in Table 29. Specimen SP27-1 used the connection configuration shown in Figure 126b, with weak washers. All other specimens used longer pins with strong washers securing the pins (see Figure 132b). The SP27-2 specimen had two 14x14 squares welded along the tube in a plane perpendicular to the one

of the connection. A design connection eccentricity of 4 mm in the plane of the connection was required for all specimens. After fabrication of specimens, imperfections were measured. They revealed that initial member imperfections were quite small: 1.19, 0.91, 2.28, 2.21 mm for SP27-1, SP27-2, SP59-1 and SP59-2 respectively. However, measured connection eccentricities were large: between -1.58 mm and +2.41 mm in the out of plane direction (+/-0.0 specified), and between -5.67 mm and +4.07 mm in the plane of the connection (+4.0 specified). This did not allow full experimental assessment of the effectiveness of design connection eccentricity. All 4 specimens were subjected to cyclic loading according to ECCS (1985) protocol. The cyclic tests consisted of four cycles in the elastic range (±0.25Dy, ±0.5Dy, ±0.75Dy and ±1.0Dy), followed by groups of three cycles at amplitudes multiple of 2Dy (3x±2Dy, 3x±4Dy, 3x±6Dy, etc.). The yield displacement Dy was determined from numerical simulations using mechanical properties of materials obtained from tensile tests. The loading was applied quasi-statically, in displacement control.

Table 29. Experimental program.

| Specimen | Pin to pin length [mm] | Cross-section | Cross section class | $\bar{\lambda}$ | Loading protocol |
|---|---|---|---|---|---|
| SP27-1 | 2700 | D139.7x6.3 | 1 | 0.75 | Cyclic, first cycle in tension |
| SP27-2 | 2700 | D139.7x6.3 with reinforcements | 1 | 0.68 | Cyclic, first cycle in compression |
| SP59-1 | 5900 | D139.7x6.3 | 1 | 1.64 | Cyclic, first cycle in tension |
| SP59-2 | 5900 | D139.7x6.3 | 1 | 1.64 | Cyclic, first cycle in compression |

The SP27-1 specimen buckled out of plane (see Figure 133) in the first cycle of 2Dy. The washers used to keep the pins into position where fixed to the pin using M6 screws. Due to out of plane buckling, the screws broke, the washers fell off, letting exterior gusset plates bend out of plane. This caused partial loss of contact between the pin and the outer gusset plates, with rapid loss of load bearing capacity of the specimen (see Figure 136).

Due to favourable initial imperfections and connection eccentricities, as well as due to the improved connection design (strong washers securing the pin) and the two 14x14 squares welded along the tube, the SP27-2 specimen buckled in the plane of the connection (see Figure 134a). Failure took place during the first tension cycle at 6Dy due to fracture of the cross section which experienced local buckling in previous compression cycles (see Figure 136).



Figure 133. Failure mode of the SP27-1 specimen.

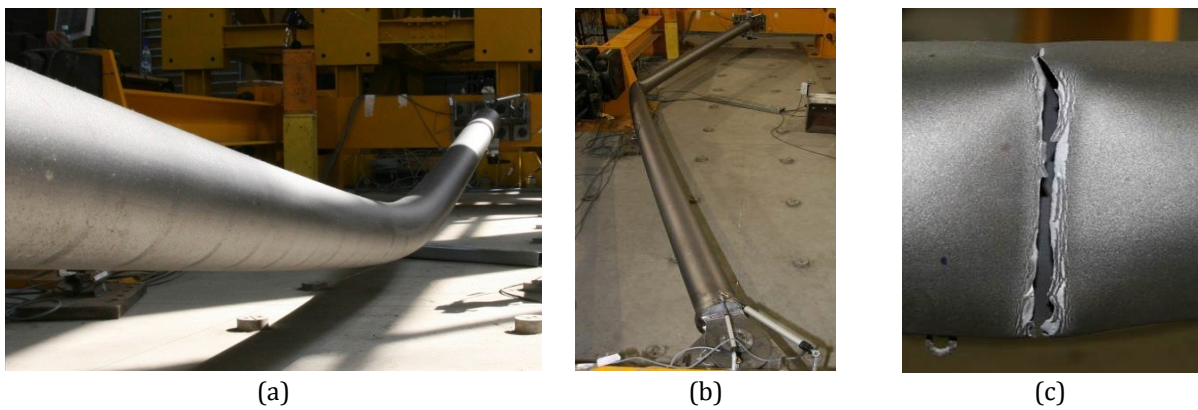Figure 134. Failure mode of the SP27-2 (a) and SP59-1 (b) specimens.



Figure 135. Specimen SP59-2: out of plane bucking (a), followed by in-plane buckling (b), and rupture of the cross-section (c).
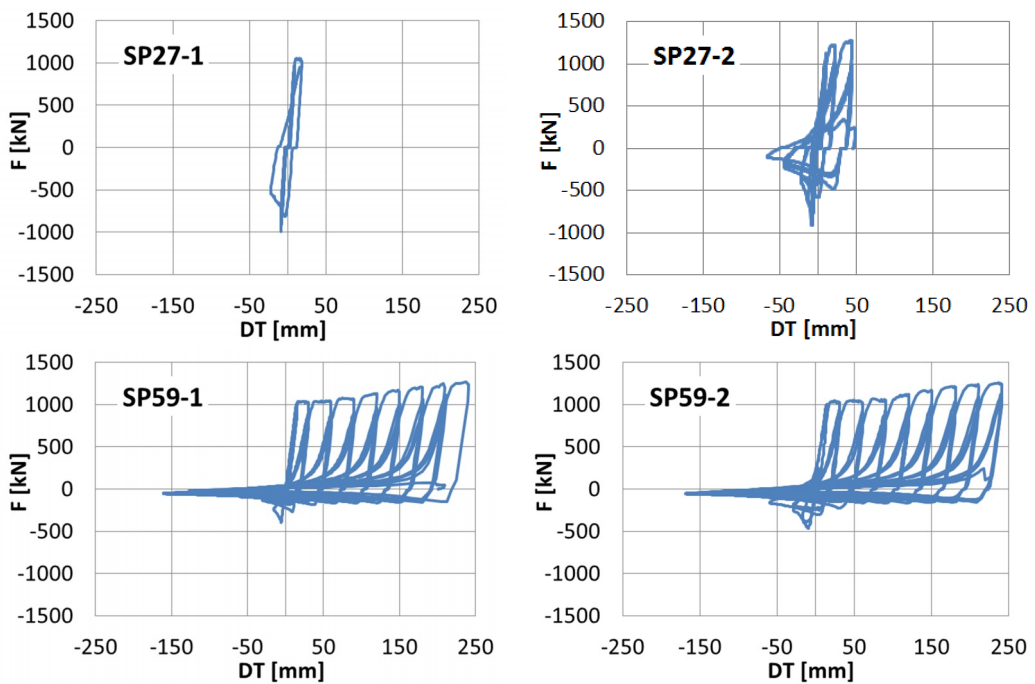


Figure 136. Force – axial deformation curves of the experimental specimens.

The SP59-1 specimen buckled in the plane of the connection, failure taking place at significant plastic deformations – 16Dy (see Figure 136). Failure was caused by fracture in tension due to progressive local buckling of the brace in compression (see Figure 134b). The SP59-2 specimen experienced similar level of plastic deformations – 16Dy (see Figure 136). However, it first buckled out of plane (see Figure 135a). However, starting with the 4Dy cycles, the buckling changed progressively to in-plane one (see Figure 135b), failure taking place similar to the previous specimen (see Figure 135c).

Welds between the tube and end plate, as well between end plate and gussets performed adequately in all cases. The cyclic response of the tubular member was similar to the one characteristic for structural hollow sections. The total ductility at fracture, $\mu_F$ (Tremblay, 2002) was considerably larger for longer braces (amounting to 4.3 for SP27-1, 9.6 for SP27-2, 26.6 for SP59-1, and 28.3 for SP59-2 specimens). Some pinching was caused by slip in the connection with pins and rotation of the eccentric pin, additionally to the one experienced due to brace buckling. Connection deformation amounted roughly to 17% and 6% of the total one for short and long specimens respectively.

Due to connection detailing and tubular shape of the cross-section, the brace assembly was shown to be sensitive to out of plane buckling, leading to failure of the connection in a brittle way. Firmly fixing the washers to the pin helps preventing brittle failure of the connection, even when buckling takes place out of the plane of the connection.

The main causes of out of plane buckling are (1) the free out of plane rotations of the connection at small deformations due to the tolerance between the pin and the hole in gussets, (2) friction that restrains to some extent in-plane rotations of the connection and (3) initial member and connection imperfections. In-plane buckling of the brace assembly is favoured by the following: (1) design in-plane connection eccentricity, (2) reduction of out of plane rotation of the connection through smaller tolerances at the pin or larger spacing between gussets, (3) lower friction at the pin – gussets interface, (4) slender braces, and (5) brace cross section with different moments of inertia about the two principal axes (elliptical, RHS, wide flange).

### 2.5.3   PUBLICATIONS

[1]   Gabor, R., Vulcu, C., Stratan, A., Dubina, D., Voica, F., Marcu, D., Alexandrescu, D. (2012). "Experimental and numerical validation of the technical solution of a brace with pinned connections for seismic-resistant multi-story structures", Proceedings of the 15th World Conference on Earthquake Engineering, September 24 - 28, 2012, Lisbon, Portugal, paper 4431.

[2]   Stratan, A., Dubina, D., Gabor, R., Vulcu, C., Marginean, I. (2012). "Experimental validation of a brace with true pin connections", Proceedings of the 7th International Workshop on Connections in Steel Structures, May 30 - June 2, 2012, Timisoara, Romania, ECCS, Dan Dubina and Daniel Grecea (Eds), ISBN 978-92-9147-114-0, pp. 535-546.

[3]   Dubina, D., Florea, D., Stratan, A., Marcu, D., Voica F. (2012). "Proiectarea asistata de experiment a structurilor complexe". AICPS Review, nr. 1-2/2012, ISSN: 2067-4546, pp. 108-122.

## 2.6 SEISMIC PERFORMANCE OF MULTI-STOREY STEEL STRUCTURES WITH FRICTION DAMPERS

The general aim of the research program was to establish the seismic performance of multistorey steel concentrically braced structures equipped with strain hardening friction damper in the braces. Recent earthquakes around the globe proved that the current degree of seismic protection is unsatisfactory and buildings suffer extensive damage or even collapse when subjected to severe or even moderate earthquake activity. As a consequence the building design codes increase seismic demands and aim to improve structural response capacity through accuracy of design and enhanced technical solutions. In current practice there are three efficient strategies to reduce seismic risk (Rai, 2000): (1) reduce seismic forces, (2) appropriate the structural response to seismic demand and (3) enhance structural damping.

Reducing seismic forces leads to capacity design of structures. Dissipative structures are designed to consume the energy induced by the seismic motion in the structure by allowing some specific elements to enter plastic domain. These dissipative elements act as fuses for the structure consuming energy, while the rest of the elements that are considered non-dissipative are designed to remain in elastic domain.

Enhancing damping strategy will imply base isolation and introduction of energy dissipation devices in the structural system. For structures isolated from seismic action and those with supplemental damping the structure is conceived as not to undergo plastic deformations by implementing devices which can absorb the seismic energy and can modify the period of vibration of the structure to more favourable values for global behaviour. In general these devices can be of three types: (1) seismic isolation devices, (2) passive energy dissipation devices and (3) active and semi-active energy dissipation devices.

Passive systems are designed to be used both for new structures and for seismic retrofit of existing structures. In general these devices function on principles such as friction between surfaces, yielding of components, and phase transformation of steel alloys, viscoelastic deformation of solids or fluids combined with the control of the flow of liquid.

Active/hybrid/semi-active control systems are an evolution of passive devices that have sensors and real time control and evaluation systems that modify partially or completely the properties of the damping devices during the recorded ground motion in order to obtain an optimal behaviour of the structure. A general classification of passive dampers might be done in reference to their governing parameter as follows:
- Velocity dependent devices - these devices are dependent of the velocity of application of the load. They modify their hysteretic behaviour according to velocity. As an example we can mention here fluid viscous dampers and fluid spring dampers.
- Displacement dependent devices - in the category enter devices with non-linear behaviour such as: steel hysteretic dampers, shape memory alloy devices, and with linear behaviour such as: elastomeric viscoelastic devices.

The research program described in the following presents the evaluation of the behaviour of a particular type of friction damper. For this purpose experimental and numerical analyses have been conducted. Based on the experimental data numerical models were calibrated and applied to evaluate the performance of concentrically braced frames equipped with such devices in the braces.

The damper studied herein is also a friction damper but has a completely different behaviour concept. The damper studied is a strain hardening friction damper with 2 distinct zones. A starting zone with low stiffness, aimed at increasing the period of vibration of the structure, and subsequently reducing the seismic forces by conducting it on the descending path of the spectrum

($T>T_C$) and a second zone with increased stiffness conceived to limit displacements for high values of seismic action (Figure 137).

The concept of this friction damper is different from "classical" friction dampers, and what is more important involves a different approach for the philosophy of dissipative structures. This was the reason which motivated the present study.

The damper dissipates energy through the elongation of a set of prestressed circular steel coils around a central steel core. The damper is characterised by 4 main parameters:
▪ Slip
▪ Stiffness of strengthening branch
▪ Maximum force
▪ Maximum stroke

The device works like a kind of mechanical telescopic device that ensures an increase in flexibility of the structure and allows energy dissipation even at small displacements avoiding the formation of plastic hinges.

Caracteristica histeretica a dispozitivului SERB-B-194C din lotul 2
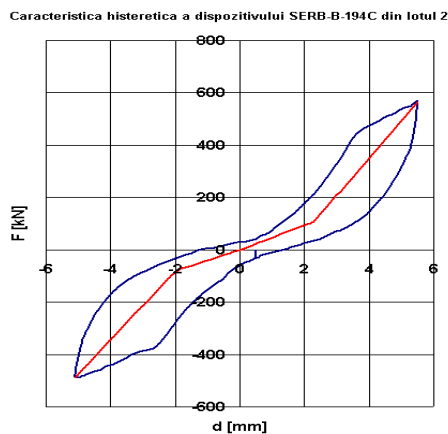


Figure 137. Hysteretic behaviour of SERB friction damper (Panait et al, 2007).

The studied damper is a Non Linear Elastic Device (NLED) according to EN 15129, 2009 that has its non-linear behaviour based on geometrical non-linear effects due to the peculiar shape of its core elements, in this case a set of steel rings sliding around a steel core, and the added friction between these elements. The increase of stiffness of the second branch classifies this damper as a Hardening Device (Figure 138). These devices can produce an increase of the initial period of vibration of the structural system due to low stiffness of the first branch but can also limit displacements in the case of earthquakes with increase in force. In addition the shape of the force displacement behaviour curve for the damper suggests a good re-centring capacity.
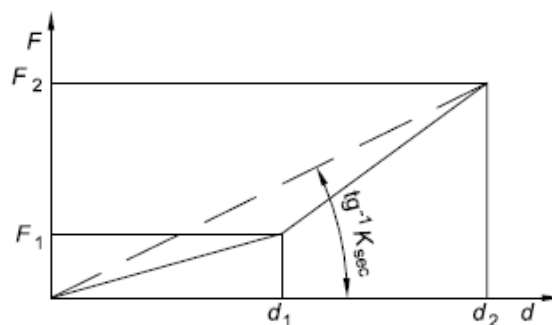


Figure 138. Hardening device (EN 15129, 2009).

The behaviour of a displacement dependent device is identified by the effective stiffness $K_{effb}$, the effective damping $\zeta_{effb}$, first branch stiffness $K_1$ and second branch stiffness $K_2$, design force $V_{bd}$ and design displacement $d_{bd}$. Force displacement capacity of the device should be able to sustain a maximum displacement or load, whichever is reached first, amplified by the reliability factor and partial factors that take into account action effects other than seismic, which can affect the initial configuration of the device (EN 15129, 2009).

## 2.6.1   EXPERIMENTAL PROGRAM

The aim of the experimental program was to evaluate and characterise the damper, in a first step, and the behaviour of the brace-damper assembly, in the second step. The first set of experimental tests was conducted on the two dampers with 1000kN and 1500KN capacity (Table 30), in order to validate their hysteretic behaviour and to ensure that the devices function in the desired parameters having a symmetric behaviour in tension and compression with stable hysteretic loops.

Table 30 Parameters for the SERB dampers tested:

| Parameters | SERB1 | SERB2 |
|---|---|---|
| Slip [mm] | 2 | 2 |
| Stiffness [kN/m] | 2x105 | 2x105 |
| Max. force [kN] | 1000 | 1500 |
| Max. stroke [mm] | +/- 15 | +/- 20 |

Data acquisition was done directly through the control and acquisition station of the machine itself without any other additional measuring instruments. Monitored parameters were total force in the damper and damper stroke. To measure the influence of the connections on the behaviour of the device the experimental test setup included the bolted end connections of the damper (Figure 139a). A cyclic load protocol with a progressive increase of force level at each step was used.
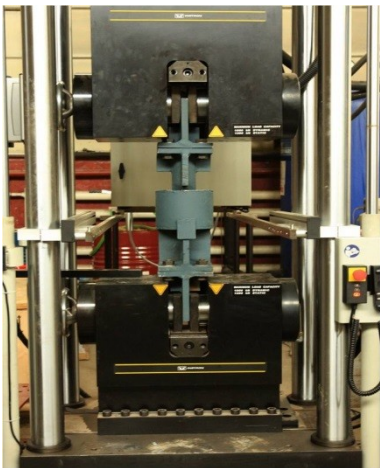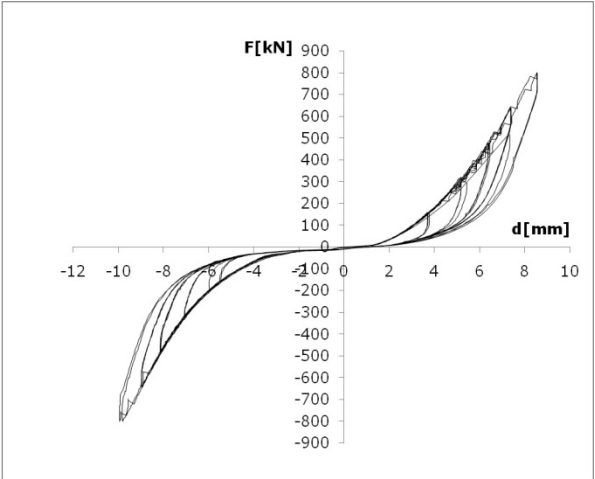


(a)                                                                 (b)

Figure 139 Experimental test setup for damper tests (a) and damper behaviour determined experimentally (b).

The hysteretic behaviour of the SERB damper obtained experimentally is presented in Figure 139b. Both devices had a similar behaviour with stable hysteretic behaviour in tension and compression.

The second set of experimental tests was conducted on the brace with damper assembly using two different concepts. A first concept is to design the braces to remain in elastic domain controlling the response of the structure solely through the friction dampers. In this case the structure has no

ductile elements and is designed with a behaviour factor corresponding to low dissipative structures of 1<q<2 and benefits from the reduction of design seismic forces due to the increase in global damping. However, introducing supplemental damping in the structure leads to a much smaller reduction of design seismic loads compared to the reduction that comes from using a higher behaviour factor value that corresponds to a dissipative design approach in which the brace itself is the main energy consuming element. For example an increase of damping in the structure to 15% critical damping leads to a reduction of the loads with only 35%. Furthermore these types of dampers have a brittle failure that must be avoided in all configurations. All the above mentioned lead to a second design concept in which the damper has sufficient overstrength compared to the brace to assure that the brace has deformation in the plastic domain and is the weaker element in the configuration. This concept should benefit in theory from both the energy dissipation capacity of the brace and the supplemental damping from the device, and the failure will occur in the brace and not in the device. For seismic motion levels corresponding to ultimate limit state the brace is the "active" element according to the dissipative design concept and for service limit state the damper is the "active" element ensuring that the brace remains in elastic domain and provides an overall damping increase. According to P100/2006 the relative story drift criteria for SLS is 0.008h, where h is the story height. For the structure analysed here this corresponds to a drift value of 28mm which leads to a displacement of 20mm in the brace. The damping devices were selected to satisfy this displacement criteria corresponding to SLS. Both design concepts presented above will be used in the configuration of the experimental tests that will be presented further on. The two design concepts will be referred to as the "Strong" brace concept and "Weak" brace concept. The experimental configuration was designed starting from the general geometry and consists of half of the beam and one of the central braces in a triangular configuration, hinged at both ends. The brace and beam assembly were rotated 90 degrees from their positioning in the frame to facilitate load application on the brace which was done through a 1000kN hydraulic actuator which was fixed on the pre-existent experimental test frame. In addition to the initial configuration presented above a secondary frame was constructed around the specimen to prevent out of plane deformation. Two profiles were attached to the front and back of the vertical beam element that ensure a 4 point contact with the two guidance beams to prevent any out of plane displacements (Figure 140). The same test setup is used both for the experimental test on braces alone and for experimental tests on brace with damper assemblies with the damper connected at the base of the brace through bolted end plates (Figure 141).



Figure 140 Experimental test setup for brace tests



Figure 141 Experimental test setup for brace with damper assembly tests

For the experimental tests on single brace and brace with damper configurations recorded parameters were: total applied force, total displacement of the specimen, relative displacement between certain predetermined points relevant for each type of test. A load protocol recommended

by European Convention for Constructional Steelworks was used (ECCS, 1985) was used. The protocol consists of a monotonic test to determine the force-displacement relationship of the specimen. With the determined values of yield displacement ($e_y$) the displacement based cyclic load protocol is constructed with one cycle at each elastic step of $0.25e_y$, $0.5e_y$, $0.75e_y$, $1e_y$ and 3 cycles at each load step multiple of $2e_y$ ($2e_y$, $4e_y$, $6e_y$, $8e_y$, etc.). The cross sections used for the brace reflect these two design concepts as follows: "strong" brace concept: HEA240 and "weak" brace concept: circular hollow section D133x5 and HEA100 profile.

Experimental tests for "weak" design concept represent the main point for the research and will be detailed in the following. The results obtained for CHS and HEA braces were very similar and it is for this reason that we will present only the experimental tests for the HEA braces with and without damper configurations. All braces without dampers were first tested monotonically to determine yield displacement and yield force needed to establish the ECCS cyclic load protocol that was later used for cyclic tests. The experimental test setup had the same general configuration for all tests and the braces were positioned with their weak axis in the plane of the test frame to ensure that buckling occurs in the vertical direction.

Force displacement curves for the HEA100 brace without dampers, obtained from monotonic tests, are presented in Figure 142. The behaviour of the HEA brace under cyclic load was very similar with the behaviour recorded for the CHS brace. At tension load cycles the brace exhibited a strength decay of approximately 20% for the second and third cycle at each load step. The brace exhibited significant stiffness degradation for each successive tension cycles. Buckling of the brace occurred for compression cycles with the formation of a plastic hinge in the middle of the brace. The first buckling of the brace was recorded at a force level of approximately 0.7 times the yield force of the brace $F_y$ and the values of the buckling force dropped continuously for the successive compression cycles that followed. The test was stopped when the values of the compression force dropped with more than 50% of maximum compression force reached. The force displacement curve recorded for cyclic tests on the HEA100 brace without damper are presented in Figure 143.
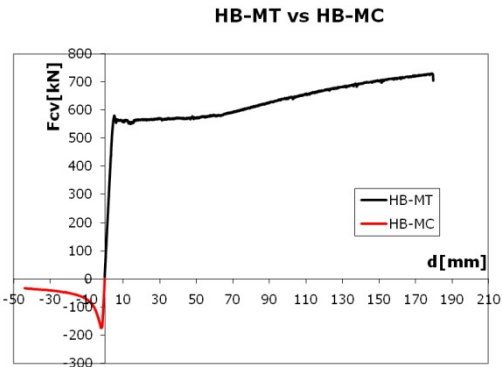


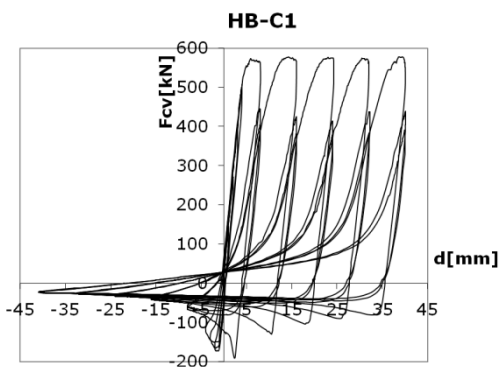Figure 142 Force displacement curves for the HEA100 brace obtained from monotonic tests

Figure 143 Force displacement curve recorded for cyclic tests on the HEA100 brace without damper

In order to analyse the influence of the damper on the global behaviour of the brace the hysteretic behaviour of the brace without damper is taken as reference curve. The behaviour of the brace with damper obtained for the two design concepts of "weak" and "strong" brace is therefore compared with the hysteretic behaviour of the brace without damper.

For the "strong" brace design concept the global behaviour of the system of brace and damper is completely governed by the constitutive law of the damper and its properties. The system does not suffer any degradation in terms of strength and stiffness these being strictly dependent on the damper properties. The system will continue to take on load until the maximum capacity of the

device is reached, with the brace remaining in elastic range. This high load carrying capacity without strength and stiffness degradation represents the advantage of this type of design concept but can also lead to an increase of the load levels in the beams and columns of the braced frame due to the pseudo-elastic behaviour of the damper. Furthermore failure of this type of system is a brittle one due to failure of the device and must be avoided.

For the "weak" brace with damper the brace is allowed to have plastic deformation and the global behaviour of the damper brace system is a mixed one. The weak element in this configuration is the brace which will ultimately fail. The behaviour of this system is presented in Figure 144 in comparison with the behaviour of the same brace, under the same load protocol but without damper. In both configurations the force level drops significantly after the first cycle at each load step and the next two cycles of the same deformation step. The brace with damper has a higher flexibility and yields at the same load step but at a displacement of approximately 50% higher. For this system up to a level of 2ey the global behaviour is governed by the behaviour of the damper and by the behaviour of the simple brace at higher load steps. The difference between these two systems can be observed more closely up to a level of two times yield deformation $e_y$ (Figure 145)
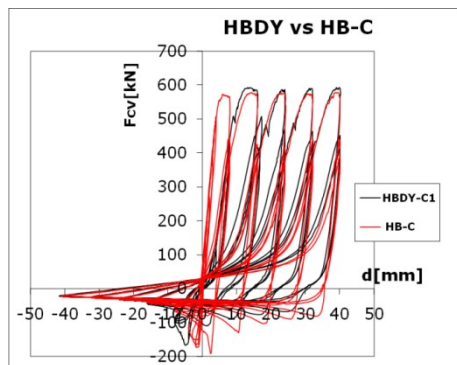


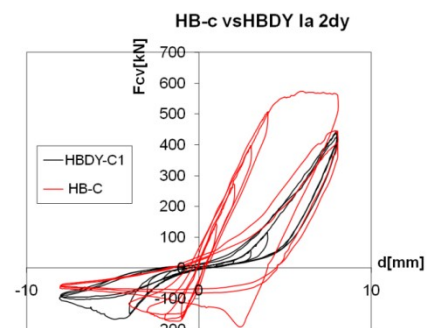Figure 144 Hysteretic behaviour of the brace with damper (HBDY) and without damper (HB-C).

Figure 145 Hysteretic behaviour at 2dy of the brace with damper (HBDY) and without damper(HB-C).

Up to this level the behaviour is that given by the damper parameters. At tension cycles the brace remains in elastic domain and the load level in the system is significantly smaller than that of the brace without damper with a higher overall flexibility. For compression cycles the brace with damper buckles at the same load level as the one without damper but has a higher deformation capacity due to the damper properties. The test was stopped when the values of the compression force dropped with more than 50% of maximum compression force reached.

The experimental results are in agreement with the two design concepts considered. For the starting load levels of up to 2$e_y$ the brace remains in elastic domain and has a lower level of energy dissipation but there is a significant decrease in load level due to the damper and also an increase in flexibility. After this level the hysteretic behaviour of the system is very similar to that of the brace without damper, with energy dissipation due to the formation of a plastic hinge in the brace. Failure in this design concept is represented by the failure of the brace in compression.

### 2.6.2   SEISMIC PERFORMANCE OF MULTISTOREY FRAMES WITH SERB DAMPERS

The main issues with modelling the behaviour of the damper are the pinching effect of hysteretic curve, stiffening behaviour ($K_2 > K_1$) and lack of degradation of the loops. For modelling of damping devices SEISMOSTRUCT software offers the use of link elements that have the possibility of defining different hysteretic behaviour for each of the 6 degrees of freedom. Several hysteretic behaviours

were tested in an attempt to model the behaviour of the SERB damper. These behaviours were defined for the degree of freedom corresponding to axial deformation having a linear elastic behaviour defined for the other 5 with sufficient stiffness to ensure their restraint. Some the trial hysteretic behaviour models were used in the first step using common behaviour curves for friction dampers. A conclusion of these trials was that to model the behaviour of the SERB damper a combination of two link elements was needed in order to obtain a larger stiffness for the second branch of the device. The final damper model was constructed using a two link elements working in parallel namely a bilinear symmetric behaviour type link (Figure 146) combined with a gap-hook element that is employed to model the pinching of the curve (Figure 147). The coupled stiffness of these two elements in parallel yielded the desired stiffness for the device.

The combined behaviour of the two hysteretic behaviours presented above is shown in (Figure 148). The damper model was compared with the behaviour obtained experimentally (Figure 149).
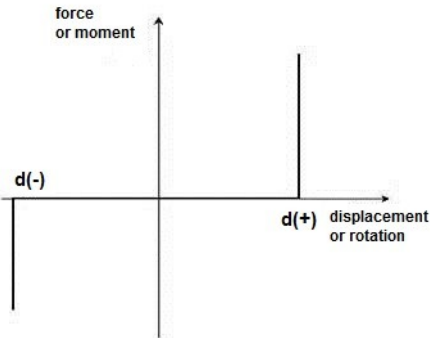


Figure 146. Gap-Hook link behaviour for damper model (Seismosoft, n.d.)
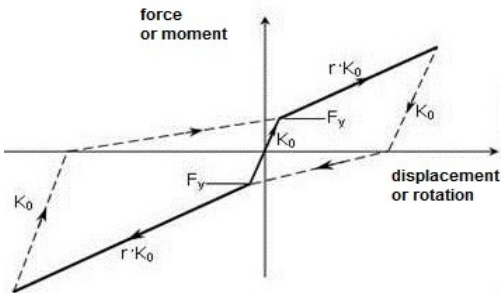
Figure 147. Bilinear Symmetric link behaviour for damper model (Seismosoft, n.d.)
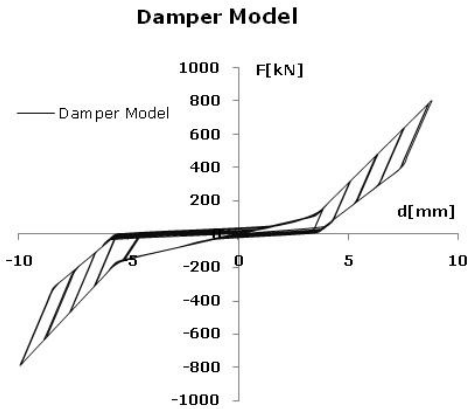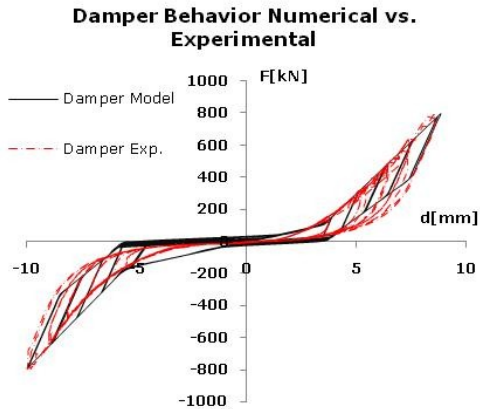


Figure 148. Behaviour of damper model.

Figure 149. Comparison between the damper behaviour of the model and the damper behaviour obtained experimentally.

Using as reference the experimental behaviour of the HEA100 brace a numerical model that could model with sufficient accuracy the cyclic behaviour of the brace was developed. The main issue that arises with brace modelling is the accurate modelling of brace buckling. For the numerical simulation SEISMOSTRUCT version5.5 Build 10 software (Seismosoft, n.d.) was used, a finite element package that uses fibre formulation. The buckling behaviour of brace was modelled using geometric imperfections computed according to EN1993 1-1 . The brace element was divided into segments with each point having corresponding values of the imperfections computed based on a

parabolic shape of the deflection with the value of the imperfection computed at midpoint of the element $e_0$ = 26.5 mm. The material model used for the steel was Menegotto-Pinto steel model with isotropic hardening, with parameters obtained experimentally from tensile tests on steel samples from the brace and calibrated parameters as follows: $A_1$=17, $A_2$=0.1, $A_3$=0.025, $A_4$=8.

A parametric study was conducted to determine the optimum number of elements in which the brace is to be divided and the value of the imperfections to be adopted comparing the cyclic behaviour of the brace with the behaviour obtained from experimental tests. The brace was divided in 2 and 4 elements and for each of the two models 4 values of the imperfections were considered: e0, e0/2, e0/3, e0/4 and length of the plastic hinge of 16.66%, 20% and 25% (Table 31).

Table 31. Parametric study to determine optimum number of elements and plastic hinge length.

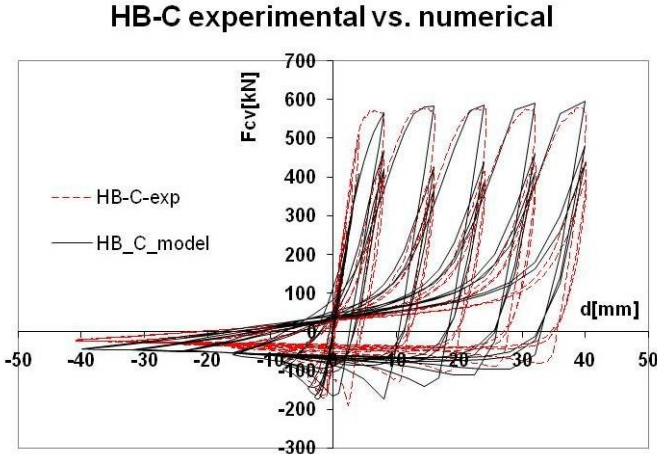| No. of elements | Imperfection | | | | Plastic hinge length |
|---|---|---|---|---|---|
| 2 | $e_0$ | $e_0/2$ | $e_0/3$ | $e_0/4$ | 16.66% |
| 4 | $e_0$ | $e_0/2$ | $e_0/3$ | $e_0/4$ | |
| 2 | $e_0$ | $e_0/2$ | $e_0/3$ | $e_0/4$ | 20% |
| 4 | $e_0$ | $e_0/2$ | $e_0/3$ | $e_0/4$ | |
| 2 | $e_0$ | $e_0/2$ | $e_0/3$ | $e_0/4$ | 25% |
| 4 | $e_0$ | $e_0/2$ | $e_0/3$ | $e_0/4$ | |



Figure 150. Comparison between cyclic behaviour of brace from the numerical model with the one obtained experimentally.
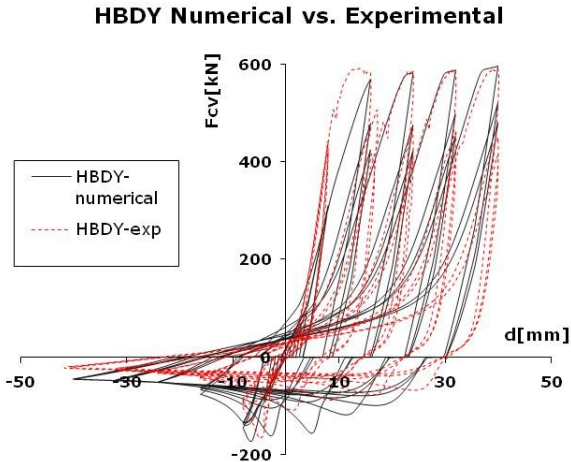


Figure 151. Comparison between numerical and experimental behaviour of brace with damper.

121

The best results were obtained for the 2 element brace with a value of imperfection at midpoint of $e_0/2$ and plastic hinge length of 20%. The behaviour of this brace model is presented in Figure 150, in comparison with the behaviour of the same brace obtained experimentally. Parametric studies conducted by Landolfo et al. (2010) also recommended the use of 2 element division for modelling cyclic behaviour of brace.

The two numerical models detailed above, calibrated on experimental test data for damper and brace were then combined to obtain the brace-damper behaviour. The results from the numerical model were compared to the experimental results (Figure 151).

The numerical model presents the same global behaviour as the one obtained from experimental data with a damper governed behaviour up to $2e_y$ and a brace governed behaviour afterwards, reaching the same peak values of force for each tension cycle and with sufficiently accurate modelling of sliding of the damper at zero force point transition. These two models for the brace and for the damper as presented above are employed in the overall assessment of the behaviour of the full frame by implementing them for studied concentrically braced frames.

The numerical model calibrated as detailed in the previous chapter is used to determine the performance of this system coupled with concentrically braced frames. The structure analysed is a 5 storey plane frame with an underground level extracted from a 3x3 layout (Figure 152) with 3 spans of 6 m with chevron bracing in the mid-span and a storey height of 3.5m (Figure 153). The frame was design according to en1993-1-1 and EN1998-1 with some special considerations from the Romanian seismic design code P100/2006considering the design spectra for Bucharest with a corner period of $T_C$=1.6s and peak ground acceleration $a_g$=0.24g.
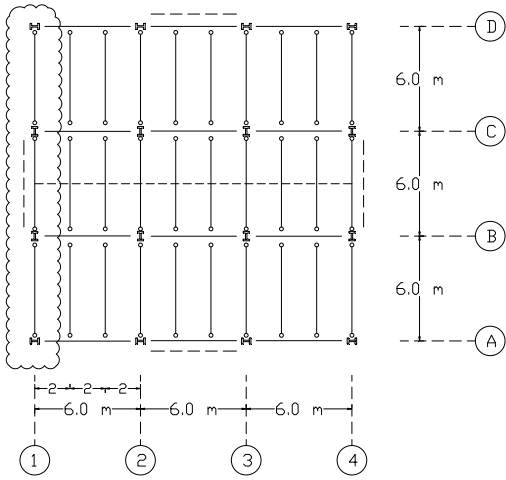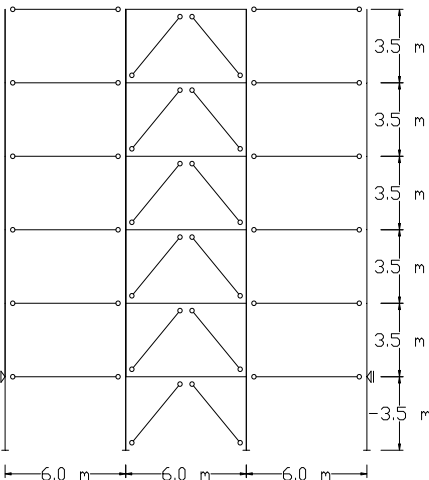


Figure 152. Plan layout.

Figure 153. Selected frame geometry.

Extensive time-history analyses were conducted using two sets of seismic motions recordings scaled to the design spectra as follows: 7 semi-artificial seismic motion characteristic for soft soil type (Bucharest) and 7 artificially generated seismic motions characteristic for stiff soil (Class B soil according to EN1998-1) both with and without dampers. The two target spectra were scaled to the fundamental period of vibration of the analysed structure, so as to yield roughly the same design seismic forces (Figure 154).

Performance based evaluation was performed using acceptance criteria for plastic axial deformation in the braces and plastic rotation for beams and columns according to FEMA356. Three performance levels were considered for each seismic motion having an acceleration multiplier of 0.5 (30 years return period), 1.0 (100 years return period), 1.5 (475 years return

period) corresponding to serviceability limit state (SLS), ultimate limit state (ULS) and collapse prevention (CP):

- SLS: $a_{g,SLS}=0.5\ a_{g,ULS}$
- ULS: $a_{g,ULS}=0.24$ g
- CP: $a_{g,CP}=1.5\ a_{g,ULS}$

Maximum drift levels (Figure 155), maximum drift at each storey (Figure 156) and top displacement for the structure (Figure 157) without dampers are presented as mean values of recorded values for all 7 seismic motions at levels corresponding to SLS, ULS and CP in comparison with the same values recorded for the structure with dampers in the braces.
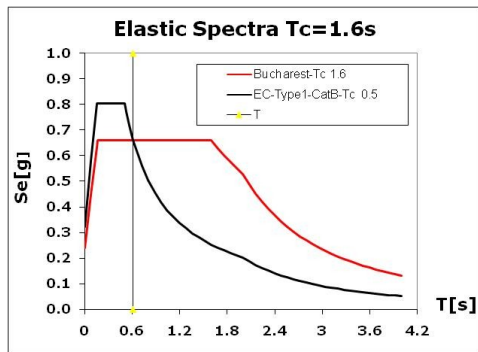


Figure 154. Elastic spectra for soft soil type ($T_C$=1.6s) and stiff soil type ($T_C$=0.5s).
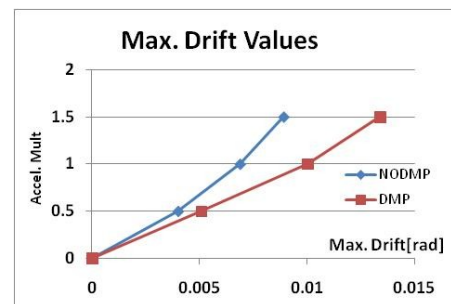
Figure 155. Maximum drift values for the structure with and without dampers (stiff soil).
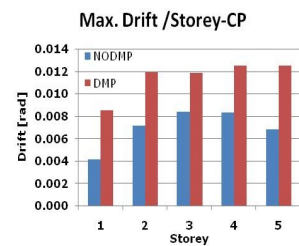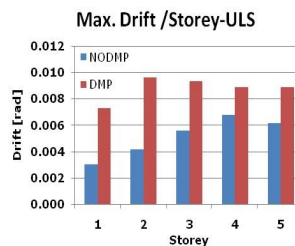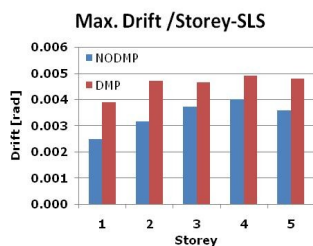


Figure 156. Maximum drift at each storey for the structure with and without dampers.
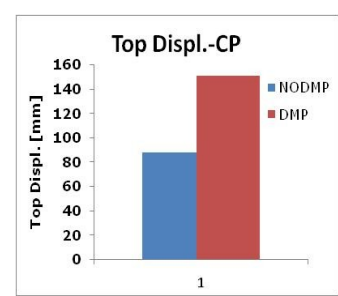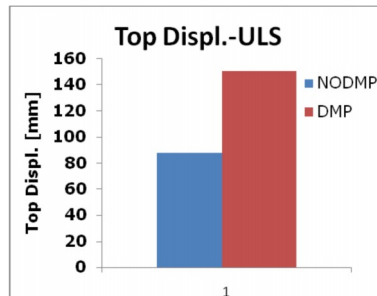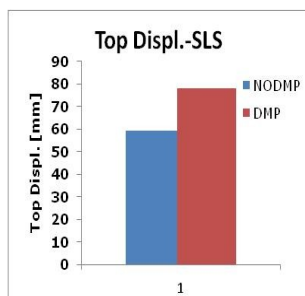


Figure 157. Top displacement for the structure with and without dampers.

At the end of each seismic recording used the structure was left to vibrate freely for 10s. Recorded values of permanent displacement at top of the structure are presented as mean values for all 7 recordings in Figure 158.

For all 7 seismic motions characteristic for stiff soil type used the results showed that for all performance levels the building with dampers exhibited an increase in drift for all 5 storeys. The

structure with dampers has lower values of permanent displacement at the top of the structure at SLS and CP.

At SLS the structure with dampers avoids almost completely the formation of plastic hinges in braces. At CP the structure with dampers has higher values of plastic deformation/rotation in elements. All plastic deformations/rotations satisfy the acceptance criteria at all levels.
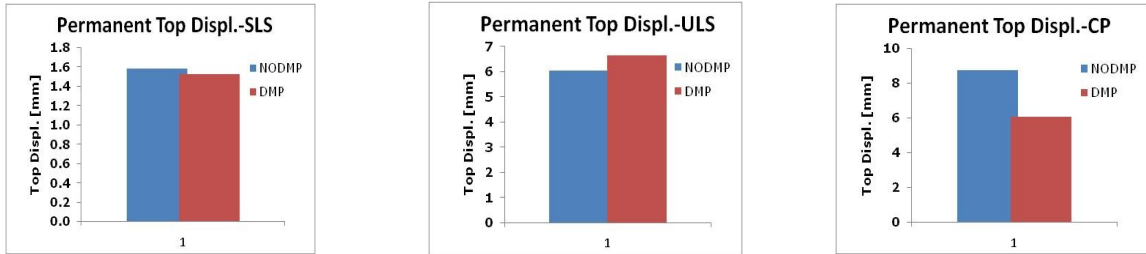


Figure 158. Permanent top displacement for the structure with and without dampers.
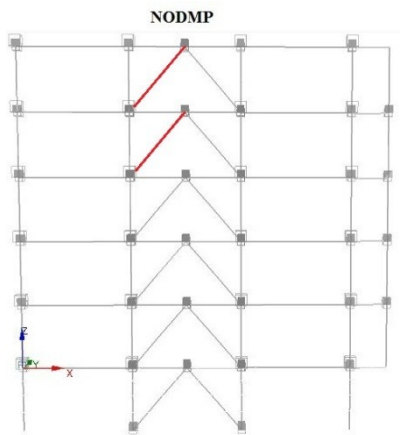


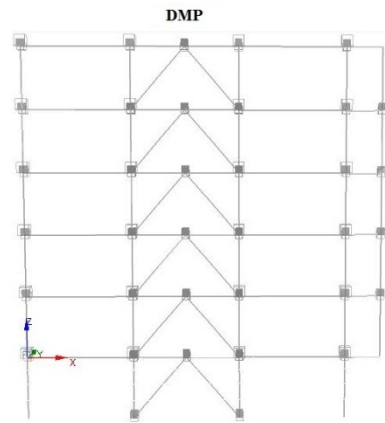Figure 159. Plastic hinge formation for CBF without dampers at SLS



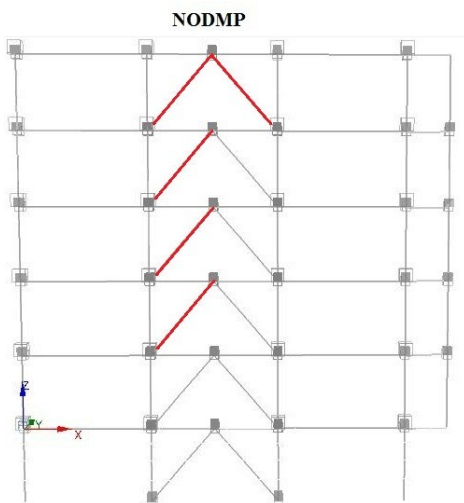Figure 160. Plastic hinge formation for CBF with dampers at SLS



Figure 161. Plastic hinge formation for CBF without dampers at ULS
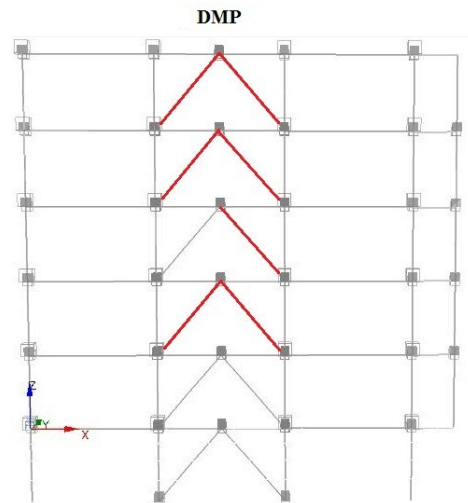


Figure 162. Plastic hinge formation for CBF with dampers at ULS

At ULS both frames with and without dampers form plastic hinges in braces (Figure 161 and Figure 162). The structure with dampers has lower values of axial plastic deformation in braces in compression but with slightly higher values for the braces in tension. At this level the structures have a similar behaviour with similar values of plastic deformation/rotation in elements. No plastic rotations of the central beams are recorded for either structure. All plastic deformations satisfy the acceptance criteria corresponding to life safety (LS) from FEMA 356. The structure with dampers has lower values of permanent top displacement then the structure without dampers.

At CP both frames with and without dampers form plastic hinges in braces and central beams. Structure with dampers has lower values of plastic axial deformation for compression braces and slightly higher for tension braces then the structure without dampers. No plastic rotations of the central beams are recorded for either structure with slightly lower values of permanent top displacement for the structure with dampers (Figure 165 and Figure 166). All plastic deformations satisfy the acceptance criteria corresponding to collapse prevention (CP) from FEMA 356.
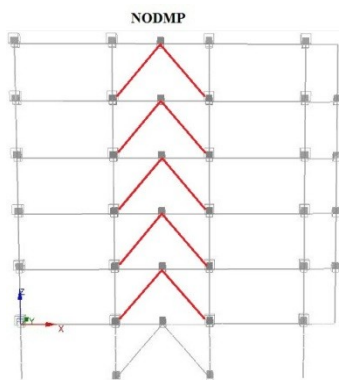


Figure 163. Plastic hinge formation for CBF without dampers at ULS
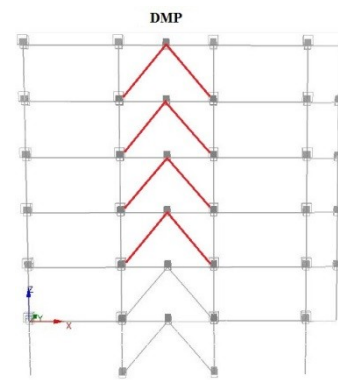
Figure 164. Plastic hinge formation for CBF with dampers at ULS

The structures with dampers were more flexible in all cases with drift levels and values of maximum top displacement higher than the ones of the structures without dampers at all performance levels. The introduction of the damper in the braces leads to a reduction of permanent drift values for structure. Plastic hinge formation in elements and the values of plastic axial deformations and plastic rotations were as follows:

- At SLS plastic hinges appear exclusively in the braces. The damper avoids almost completely the formation of plastic hinges in braces keeping the structures in elastic domain.
- At ULS plastic hinges are limited to braces for both structures. The structures with and without dampers have a similar behaviour with values of all plastic axial deformation that satisfy the acceptance criteria for LS.
- At CP, for the CBF frame, plastic hinges form only in braces with only a few exceptions when plastic rotations are recorded in central beams but with very low values.

As a conclusion this type of damper is efficient in reducing the seismic response of a building for earthquakes characterized by short corner period $T_C$=0.5s (stiff soil) by preventing the formation of plastic hinges at SLS and reducing the permanent displacement of the structure. For earthquakes characterized by long corner period $T_C$=1.6s (soft soil) this type of damper is not effective in improving the behaviour of the structure. Under this type of seismic motions the structures with dampers form plastic hinges in non-dissipative elements with values that exceed the acceptance criteria for the corresponding performance levels.

## 2.6.3 PUBLICATIONS

[1] Filip-Vacarescu, N., Stratan, A., and Dubina, D. (2014). "Experimental validation of a strain hardening friction damper". Proceedings of the Romanian Academy Series a - Mathematics Physics Technical Sciences Information Science, 15(1), 60-67.

[2] Filip-Vacarescu, N., Stratan, A., and Dubina, D. (2014). "Seismic performance of multistorey steel frames with strain hardening friction dampers". Proceedings of the Romanian Academy Series a - Mathematics Physics Technical Sciences Information Science, 15(2), 174-181.

[3] Filip-Vacarescu, N., Stratan, A., and Dubina, D. (2011). "Behavior of concentrically braced frames with friction dampers." Pollack Periodica, 6(1), 59–71. Paper ISSN: 1788-1994, Online ISSN: 1788-3911.

[4] Norin Filip-Vacarescu, Aurel Stratan, Dan Dubina, Application of strain hardening friction dampers in concentrically braced frames, BULLETIN OF THE TRANSILVANIA UNIVERSITY OF BRASOV, CNCSIS B+, Brasov, ISSN 2065-2127, 2012, CD, CD, Bulletin of the Transilvania University of Brasov, Series I Engineering Sciences, International Scientific Conference CIBv2012.

[5] Norin Filip-Văcărescu, Aurel Stratan, Dan Dubină (2011). "Cadre metalice contravântuite centric dotate cu amortizori cu frecare", AICPS Review, nr. 1-2/2011, p. 184-197. ISSN: 2067-4546

[6] Filip-Vacarescu N., Stratan A., Dubina D. (2011). "Behavior of concentrically braced frames with friction dampers". COMPDYN 2011, 3rd ECCOMAS Thematic Conference on Computational Methods in Structural Dynamics and Earthquake Engineering M. Papadrakakis, M. Fragiadakis, V. Plevris (eds.) Corfu, Greece, 25–28 May 2011, pp. 2793-2807.

[7] Filip-Văcărescu, N., Stratan, A., Dubină, D. (2013). "Sisteme structurale disipative cu contravântuiri cu amortizori cu frecare: studiu de souţie şi comparaţie cu sistemele convenţionale". A XIII-a Conferinţă Naţională de Construcţii Metalice, Bucureşti, 21–22 noiembrie 2013, Editori: Daniel Bîtcă şi Paul Ioan, pp. 141-156, ISBN 978-973-100-306-1.

[8] Filip-Vacarescu, N., Stratan, A., and Dubina, D. (2011). "Behaviour of Concentrically Braced Frames with Friction Dampers", EUROSTEEL 2011, August 31 - September 2, 2011, Budapest, Hungary, p. 987-992. ISBN: 978-92-9147-103-4.

[9] Filip-Văcărescu, N., Stratan, A., Dubina, D. (2010). "Cadre metalice contravântuite centric dotate cu amortizori cu frecare". Lucrările celei de-a 12-a Conferinţe Naţionale de Construcţii Metalice "Realizări şi preocupări actuale în ingineria construcţiilor metalice", Timişoara, 26-27 noiembrie 2010, Dubina, Ungureanu, Ciutina (Ed.), Editura Orizonturi Universitare, p. 221-232. ISBN: 978-973-638-464-6.

[10] Filip-Vacarescu, N., Stratan, A., Dubina, D. (in print). "Evaluation of dissipative effectiveness of a hybrid system composed by a buckling restrained brace with a magneto rheological damper", 8th International Conference on Behavior of Steel Structures in Seismic Areas STESSA 2015, Shanghai, China, July 1-3, 2015. Paper no. 121.

## 2.7 PREQUALIFICATION OF BOLTED BEAM TO COLUMN JOINTS WITH HAUNCHES

The use of pre-qualified joints is a common practice in U.S. and Japan. Nevertheless, the standard joints pre-qualified according to codified procedures in U.S. and Japan cannot be extended to Europe, due to differences in materials and section shapes. Moreover, the beam-to-column joint types usually adopted in U.S. and Japan are not commonly used in Europe. As a result, the existing scientific and technical background on pre-qualification may not be directly extended to European context. For this reason, a European research project entitled European pre-QUALified steel JOINTS (EQUALJOINTS), is currently underway and aims at seismic pre-qualification of several beam-to-column connection typologies common in the European practice, and which are illustrated in Figure 165. In particular, the research activities will focus on the standardization of design and manufacturing procedures based on different geometric and mechanical parameters of selected joint typologies. Hence, a large experimental programme supported by theoretical and numerical analyses is proposed to provide reliable standard joints that can be easily used by designers.
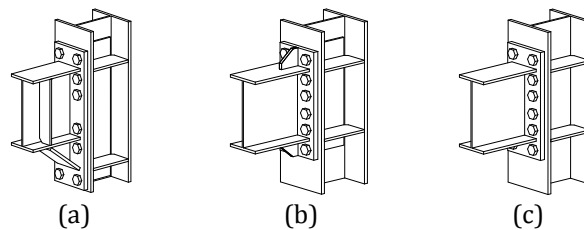


Figure 165. Connection typologies with: (a) haunches, (b) stiffened end-plate, (c) un-stiffened end-plate.

### 2.7.1 EXPERIMENTAL PROGRAM

The aim of the experimental program at the Politehnica University of Timisoara is to investigate the behaviour of bolted connections with haunches under monotonic and cyclic loading. A set of 24 beam-to-column joint assemblies will be tested in order to evaluate different parameters that are specific for this type of connection. Single sided and respectively double sided joints were selected from moment resisting frames (MRF) as illustrated in Figure 166.
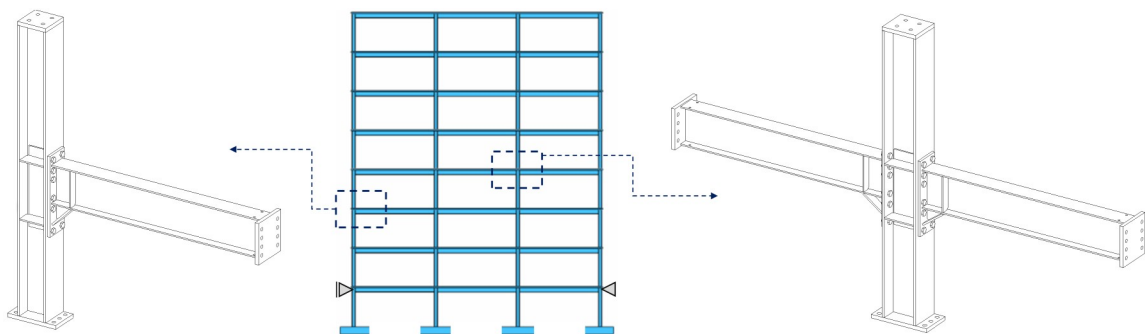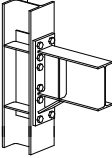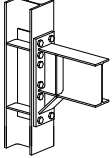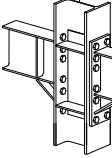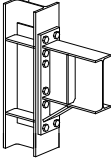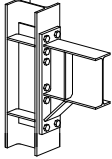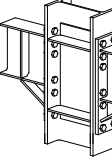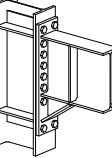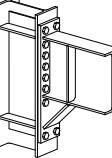


Figure 166. Single-sided and double-sided joints selected from MRF structure.

The experimental program, summarized in Table 32, contains three groups of specimens:
- Group 1: full strength & rigid connection, shallow haunch (35° angle), strong web panel;
- Group 2: full strength & rigid connection, steep haunch (45° angle), strong web panel;
- Group 3: full strength & semi–rigid connection, shallow haunch (35° angle), balanced web panel.

127

Table 32. Experimental program on bolted beam-to-column joints with haunches.

| Group 1: single-sided joints | Group 2: single-sided joints | Group 3: double-sided joints |
|---|---|---|
| EH1-TS-35 IPE 360 HEB 280 | EH1-TS-45 IPE 360 HEB 280 | EH1-XB-35 IPE 360 HEB 340 |
| EH2-TS-35 IPE 450 HEB 340 | EH2-TS-45 IPE 450 HEB 340 | EH2-XB-35 IPE 450 HEB 500 |
| EH3-TS-35 IPE 600 HEB 500 | EH3-TS-45 IPE 600 HEB 500 | |

Group 1 and Group 2 serve for qualifying two alternative haunch geometries (lower and upper limit of reasonable haunch angle) for considered range of beam size. Group 3 investigates joints with balanced panel zone strength, but which are semi–rigid connections. Two supplementary web plates are used for the joints of Group 1 and Group 2, while for Group 3 only one supplementary web plate is used. Additionally, larger column depth increases the range of prequalified column sizes. The complete parameters considered within the experimental program are: loading protocol (monotonic and cyclic), member size, single-sided and double sided connections, strong panel zone / balanced panel zone, strong beam and haunch geometry. It is to be mentioned that the experimental program will be extended through numerical simulations with the aim to investigate additional parameters as well.

## 2.7.2   PRE-TEST NUMERICAL SIMULATIONS

The pre–test numerical simulations were realised with the aim to obtain an accurate prediction for response of the beam-to-column joint assemblies, and in particular considering the following objectives: (i) to avoid unacceptable failure during the tests, (ii) to validate the analytical design procedure.

The numerical simulations were performed with the finite element modelling software Abaqus. In brief, the modelling procedure was realised considering: solid linear hexahedral elements of type C3D8R, dynamic explicit type of analysis (due to large contact surfaces), contact between end-plate and column flange defined through a normal (hard contact) and tangential (penalty with friction) interaction law, and the load was applied through a displacement control. In addition, the material properties for bolts were calibrated based on data from a past project (Dubina et al., 2015), in which extensive experimental investigations were performed on T-stubs.

Figure 167a shows the material model considered for bolts and for the longitudinal and transversal plates of the investigated T-stub. It is to be noted that the material model is represented in terms of true stress – true strain relationship. In addition, Figure 167b shows the comparison between test and simulation for a T-stub configuration which was designed considering a Mode 2 close to Mode 3 failure, in which Mode 2 is characterized by the failure of the bolts and yielding of the flange, and Mode 3 is characterized by the failure of the bolts. As can be observed, the numerical model of the T-stub was able to reproduce with good accuracy the response of the tested T-stub in terms of force–displacement curve. Consequently, the initial stiffness and the ultimate capacity were in good

agreement with the test, as well as the loss of capacity at 8.75 mm displacement, corresponding to failure of the bolts.

The calibrated material model of the bolts was further used in the FE joint models developed with the aim to investigate the response of the designed bolted beam-to-column joint assemblies under monotonic (sagging and hogging bending moment) and cyclic loading.



(a)          (b)
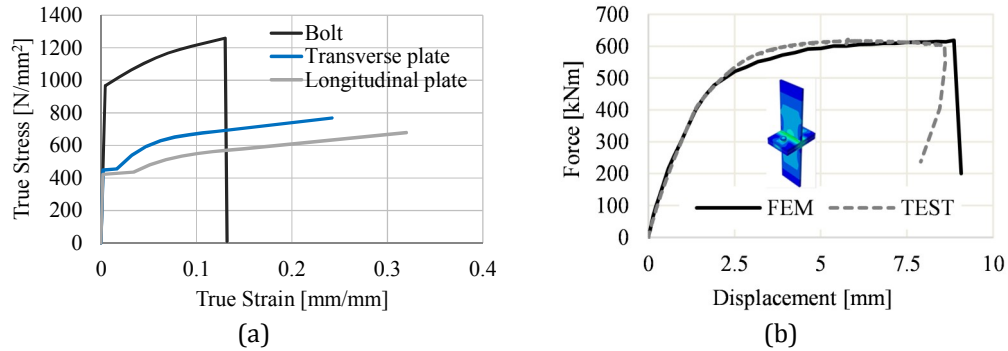
Figure 167. Calibration of numerical model of T-stub: (a) material model, i.e. true stress – true strain relationship for bolts (calibrated) and for longitudinal and transversal plates (from material sample tests), (b) comparison between test and simulation (T-stub) in terms of force-displacement relationship.

The analytical design procedure of the bolted connections with haunches was developed based on the component method implemented in EN 1993-1-8. In brief, the design of the joints was performed considering the formation of the plastic hinge in the beam (near to the haunch). Further, the components of the joint were designed and/or checked so as to comprise an equal or higher capacity in comparison to the fully yielded and strain hardened plastic hinge (Maris et al., in print). It is to be noted that the conventions of the component method assume that basic components of the connection, i.e. end-plate, web panel, beam flange and column flange, possess certain ductility and for this reason a plastic distribution of internal forces can be assumed. In addition, a common assumption of the method considers the centre of compression located in the middle of the beam flange (sagging bending moment), and respectively in the middle of the haunch flange (hogging bending moment). Consequently, an important issue was to determine the actual value of forces in active bolt rows and the lever arm corresponding to each bolt row.



(a)          (b)          (c)
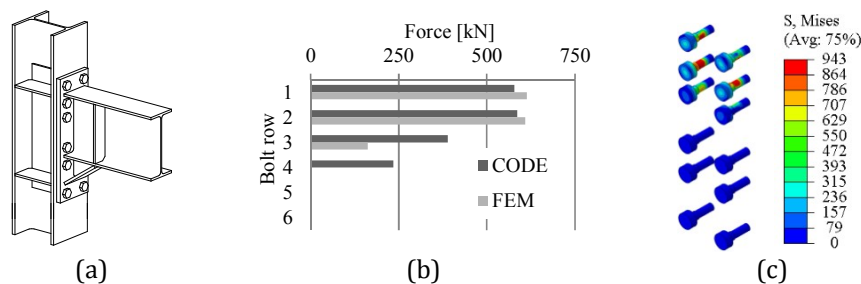
Figure 168. (a) EH1-TS35 joint, (b) active bolts under hogging moment, (c) von Misses stress distribution in the bolts.

Numerical models were developed for each beam-to-column joint configuration of the experimental program (see Table 32). Further, the joint models were analysed under monotonic loading, considering both sagging and hogging bending moment in the beam. The results of the numerical simulations confirmed the intended failure mode, i.e. formation of the plastic hinge in the beam (see Figure 171). In addition, it was found that the active bolt rows were those situated near the flange in tension as can be observed in Figure 168 for EH1-TS35 joint. Figure 168b shows a comparison

129

between the capacities of the specific bolt rows computed based on EN 1993-1-8 code provisions, and the actual forces which developed in the corresponding bolt rows. As can be observed, even though the bolt row number 3 and 4 has a significant capacity according to the code provisions, in the FE model these are not active.

The actual distribution of forces within the bolt rows can be justified by the stiffness of the end-plate and the small plastic deformation within bolts (i.e. plastic strain in amount of 2.5%). Furthermore, it was observed that the location of the compression centre was shifted inside of the connection. Figure 169a shows the pressure areas at the interface between end-plate and column flange. It was found that the compression centre was located at a distance equal to 60% of the haunch depth measured from the bottom flange of the beam as can be seen in Figure 169b.
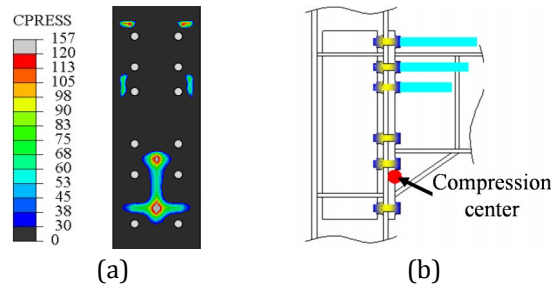


Figure 169. Compression surfaces (a), force distribution in bolts and position of centre of compression (b).

Based on the outcomes of the FE simulations, the design procedure was adjusted considering the actual position of the compression centre and the active bolt rows. As a result, each beam-to-column joint configuration of the experimental program (see Table 32) was re-designed and investigated through FEM.

The pre-test numerical simulations carried out on the designed beam-to-column joint assemblies allowed investigating the influence of several parameters, i.e. influence of: member size, haunch geometry, thickness of haunch flange, column web panel strength, and cyclic loading. Accordingly, the pre-test numerical program consisted of extensive investigations for which only a brief presentation is possible herein.

The influence of member size was investigated considering three cross-sections for both members of the joint assemblies according to the experimental program described in Table 32. Consequently, the numerical simulations evidenced higher values of equivalent plastic strain (PEEQ) corresponding to beams of larger cross-sections and at the same rotation (i.e. 40 mrad). Figure 170a shows the moment–rotation curve for the three joint configurations of Group 1 (see Table 32). In addition, it was observed that the centre of the plastic hinge was situated at a distance equal with 20% of the beam depth measured from the end of the haunch (see Figure 170b). It is to be noted that initial imperfections were not considered within joint models. For this reason the ultimate capacity of the beams are higher than the expected bending capacity of the beams. Table 33 summarizes the PEEQ values for each joint configuration of Group 1 and Group 2, corresponding to 40 mrad rotation obtained under hogging and sagging bending moment. The beams are made of S355 steel grade, and the cross-sections are class 1. It is to be noted that the material model used in simulations was based on the nominal properties of the steel grade, which were affected (multiplied) by the overstrength factor ($\gamma_{ov}$=1.25), justified by the actual properties of steel grades (higher than nominal values).

The influence of haunch geometry was investigated considering various angles ranging between 30° and 50°. The optimum results were obtained for angles between 35° and 45°. The depth of the haunch included values of 45% up to 55% of the beam depth. The study revealed that the capacity and the initial stiffness of the connection increased for upper values of the haunch angle and depth.

However, from architectural reasons and from the economical point of view, the minimum haunch depth and a smooth slope are recommended. The influence of the column web panel strength is one of the parameters of the experimental program (see Table 32). Accordingly, Group 1 and Group 2 are characterised by a strong web panel, while the joint configurations within Group 3 have a balanced web panel zone. Based on FEM results, Figure 171 shows the ratio between von Misses stress and yield strength, measured within the column web panel corresponding to a 40 mrad rotation. As can be observed, the single sided connections, i.e. EH1-TS35 and EH2-TS35, have a 25% strength reserve, while the double sided connections, i.e. EH1-XB35 and EH2-XB35, exceed by 5% the yield strength. However, corresponding to a rotation of 65 mrad (equivalent to the expected bending capacity of the beam), the plastic deformation of the column web panel is higher for double sided joints. It is to be noted that the double sided joints were design to be full strength and semi-rigid joints with balanced column web panel. Consequently, plastic deformations were developed in the panel zone and the total rotation of the joint assembly was affected, but in a low amount.



(a)                                                         (b)
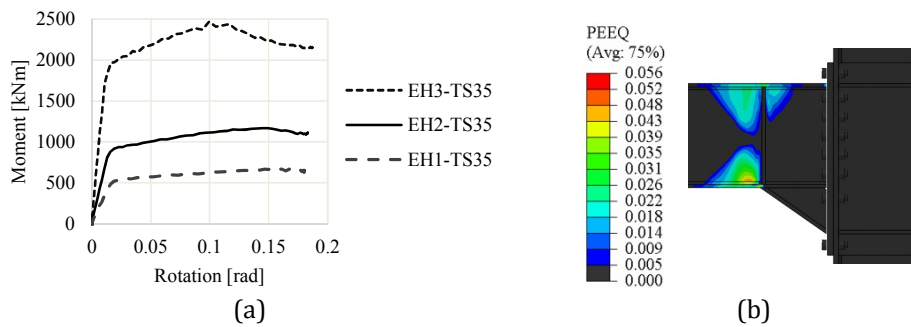
Figure 170. Moment-rotation curves (a), PEEQ for EH2-TS-45 hogging moment (b).

Table 33. Equivalent plastic strain (PEEQ).

| Joint configuration | EH1-TS35 | EH2-TS35 | EH3-TS35 | EH1-TS45 | EH2-TS45 | EH3-TS45 |
|---|---|---|---|---|---|---|
| Hogging moment | 3.8% | 4.3% | 5.6% | 3.4% | 4.3% | 5.3% |
| Sagging moment | 3.6% | 4.3% | 5.4% | 3.6% | 4.3% | 5.1% |
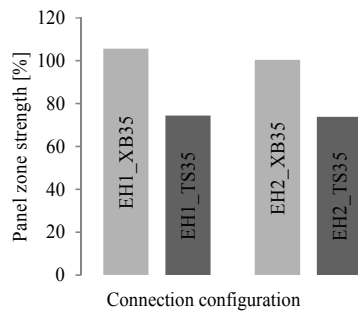


Figure 171. Ratio between von Misses Stress and yield strength fy=355 MPa.

According to EN 1998-1 the contribution of the panel zone to the total joint rotation must be limited to 30% of total joint rotation. Consequently, the aim of this investigation was to analyse the influence of the panel zone to the total joint rotation. Figure 172 shows the moment rotation curves and equivalent plastic strain corresponding to EH2-TS35 and EH2-XB35 joints. An increase of strength can be observed for EH2-XB35 connection due to the change of the column cross section from HEB 340 to HEB 500. The weakest component for the connection was the column flange in bending. For double sided connection the PEEQ deformations in the beams are smaller due to distribution of the plastic strain in column web panel.
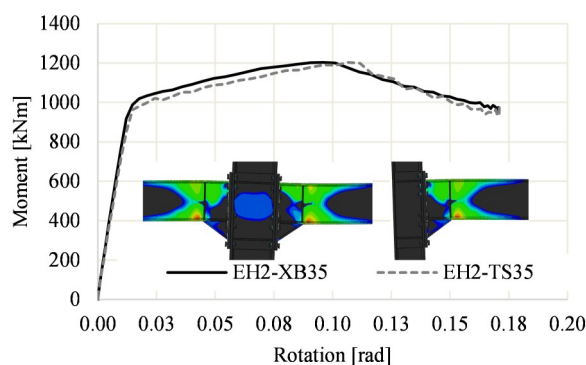
Figure 172. Moment rotation curves and plastic deformations corresponding to EH2-TS35 and EH2-XB35 joints.

In addition to the previous parameters, pre-test numerical simulations included also the investigation of the joint response under cyclic loading conditions. On this matter, it is to be noted that the difference between the monotonic and cyclic investigation of a joint model is mainly related to the loading procedure and the material model (corresponding to the dissipative zone). Regarding the loading procedure, a smooth cyclic loading pattern was used based on the ANSI/AISC 341 loading protocol, which was characterized by two cycles for each of the following amplitudes: 10, 15, 20, 30, 40, 50 mrad.

In relation to the material, several models are available in Abaqus, i.e. with isotropic, kinematic, or combined isotropic-kinematic hardening model. Under monotonic loading conditions, the isotropic model can be adopted for steel components. For this purpose, the true stress – true strain curve can be used as input. Under cyclic loading conditions, the combined isotropic-kinematic hardening model is more suitable, and therefore, it was used in the current study. The input for the material model was represented by the yield strength of the steel part, and in addition the cyclic hardening parameters as given by Dutta et al. (2010), i.e. $C_1=42096$, $\gamma_1=594.45$, $Q_\infty=60$, $b=9.71$.

The results from the cyclic analysis of the EH2-TS-35 joint configuration are shown in terms of moment-rotation curve computed at column centreline, von Misses stress distribution and equivalent plastic strain within the joint assembly (see Figure 173).
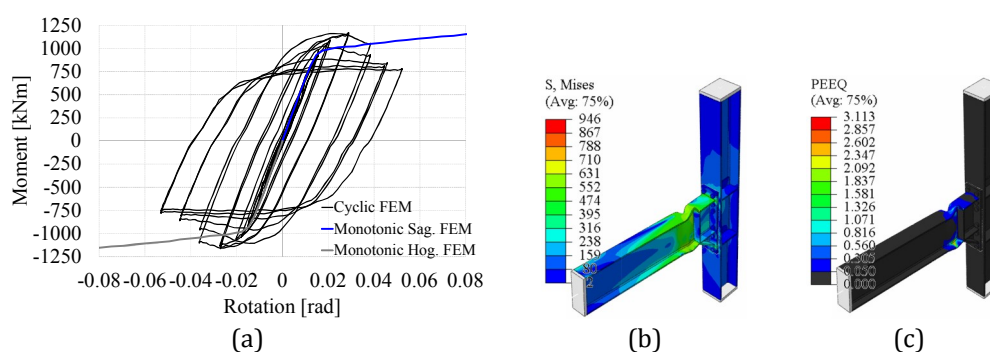


Figure 173. Cyclic response for EH2-TS-35: (a) moment-rotation curve (monotonic and cyclic loading conditions), (b) von Misses stress distribution, (c) equivalent plastic strain.

As can be observed, under cyclic loading conditions, large plastic deformations developed in the beam (dissipative zone), while the bolts were characterised by elastic response with local minor plastic deformations. In addition, the moment rotation curve evidenced an increase of capacity (see cycles of 20 and 30 mrad amplitude), compared to the monotonic response, and further the capacity decreased (see cycles of 40, 50 and 60 mrad amplitude).

The seismic performance of the joint was evaluated by constructing an envelope curve through the peak values of the first cycle for each amplitude, and further the rotation of the joint assembly was obtained from the intersection of the envelope curve with the horizontal line representing the 20% reduction of the capacity with reference to the maximum bending moment. Consequently, a rotation of 41 mrad was obtained, which is higher than the 35 mrad limit from EN 1998-1, and therefore the seismic performance of the joint was considered acceptable.

The pre-test numerical simulations carried out for the joint assemblies designed based on EN 1993-1-8 confirmed the intended failure mode, i.e. formation of the plastic hinge in the beam close to the haunch ending. However, other assumptions considered in design were not confirmed, in particular: force distribution in the bolt rows, and position of the compression centre (middle of the compressed haunch flange). In contrast, the active bolt rows were those situated near the flange in tension, and the compression centre was located at a distance equal to 60% of the haunch depth measured from the bottom flange of the beam. As a result, the design procedure was adjusted and the beam-to-column joint configurations were re-designed and analysed.

The parametric study allowed investigating the influence of: member size, haunch geometry, web panel strength, and cyclic loading. Consequently, the study evidenced higher strain in members (beams) of larger cross-section, for the same joint rotation. In addition, the capacity and the initial stiffness of the connection increased for higher values of haunch angle and depth, but for economic and architectural reasons, haunches with minimum depth and a smooth slope are recommended.

Finally, the joint response was evaluated under cyclic loading conditions, which lead to an increase of capacity corresponding to the cycles of 20 and 30 mrad amplitudes. For higher amplitudes, the capacity decreased compared to the monotonic curve due to local buckling of flanges and web under compression. In addition, the seismic performance was evaluated constructing an envelope curve through the peak values of the first cycle for each amplitude, and further the rotation of the joint assembly was obtained from the intersection of the envelope curve with the horizontal line representing 20% reduction of the maximum capacity. Consequently, a rotation of 41 mrad was obtained, which is higher than the 35 mrad limit from EN 1998-1, and therefore the seismic performance of the joint was considered acceptable.

### 2.7.3   PUBLICATIONS

[1]    Dubina, D., Stratan, A., Maris, C., Marincu, A. (2014). "Precalificarea îmbinărilor structurilor în cadre metalice amplasate în zone seismice – proiect european". AICPS Review, nr. 1-2/2014, ISSN: 2067-4546, pp. 207-216.

[2]    Maris, C., Vulcu, C., Stratan, A., and Dubina, D. (2014). "Numerical Simulations of Bolted Beam to Column Connections with Haunches in Steel Moment Frames." Proceedings of the Second International Conference for PhD Students in Civil Engineering and Architecture, UTPRESS, Cluj-Napoca, Romania, 109–116.

[3]    Maris, C., Vulcu, C., Stratan, A. and Dubina, D. (in print). "Experimental program and numerical simulations of bolted beam to column joints with haunches", 8th International Conference on Behavior of Steel Structures in Seismic Areas STESSA 2015, Shanghai, China, July 1-3, 2015. Paper no. 110.

# 3 PROFESSIONAL DEVELOPMENT PLAN

## 3.1 SCIENTIFIC DEVELOPMENT PLAN

As shown in section 1.1, the subject of "re-centring eccentrically braced frames" has a central place in the past achievements of the author. It gradually evolved from a conceptual idea developed within the PhD thesis into a solid development supported by extensive numerical simulations and large-scale tests. One last step is missing: implementation into practice. As a short-term objective, the author intends to coordinate development of design guidelines, in a cooperative effort by the research team from the Politehnica University of Timisoara (Romania), Joint Research Centre (JRC) in Ispra (Italy), and University of Naples Federico II (Italy). In order to promote the outcomes of the pursued research, it is intended to organise a workshop at the JRC Ispra. The medium-term objective is to implement this design concept into a practical application, and promote the innovative design approach to structural designers. The long-term objective is to extend the concept of **"re-centring structures"** to other structural typologies, such as dual Buckling-Restrained Frames (BRBFs) and Steel Plate Shear Walls (SPSWs).

The Laboratory of Structures from the department of Steel Structures and Structural Mechanics offers a large set of high-end testing equipment. Large-scale testing is currently supported by four quasi-static actuators, a reaction frame, a reaction wall and a strong floor. Upgrading of testing facilities is currently underway with two high-capacity quasi-static actuators, two dynamic actuators, hydraulic power supply and a shaking table, among others. The vast majority of seismic-related structural testing that has been performed until now was quasi-static tests on components (e.g. beam to column joints), using standardised and pre-determined cyclic loading protocols. Though technically possible, pseudo-dynamic testing, that combines experimental testing with computer simulation of dynamic response has not been implemented up to date in the laboratory of Steel Structures. This experimental technique offers the advantage of realistic seismic simulation on large-scale structural models, when strain-rate effects are not important. Therefore, **"implementation of pseudo-dynamic testing technique"** represents the next target of the author. At the same time, development of **"testing techniques for shaking table tests"** will be addressed, in order to fully utilize the experimental potential of the laboratory. Though the dimensions of the shaking table (1.5x1.5 m) will allow only reduced-scale dynamic tests, they are mandatory for testing systems that use-strain-rate or velocity dependent devices, such viscous dampers, magneto-rheological devices, etc.

Another research direction that is targeted by the author is **"Buckling Restrained Braced Frames (BRBFs)"**. They represent a promising structural typology that has been extensively used in the Unites States and Japan, but has a very limited application in Europe. One of the main impediments is lack of design guidelines, "know-how", and the need for experimental qualification of the dissipative devices. Design guidelines for BRBFs have been recently introduced in the Romanian seismic design codes, the other problems still remain. A project coordinated by the author (contract no. 99 / 2014, PN-II-PT-PCCA-2013-4-2091: 2014-2016 "Implementarea în practica de proiectare anti-seismică din România a contravântuirilor cu flambaj împiedicat – IMSER – Implementation into Romanian seismic resistant design practice of buckling restrained braces" is currently underway. It will support the development of two types of BRB devices: classical and "dry", prequalification of a set of common-capacity devices and development of design guides for fabricators and designers.

A further research direction that the author intends to develop is the **"seismic protection of buildings using passive and semi-active control"**. A particular type of semi-active device, based on magneto-rheological fluids is currently under investigation by the author as part of the research

team of the contract no. 77 / 2014 PN-II-PT-PCCA-2013-4-1656: 2014-2016 "Protectia seismică a structurilor cu sisteme de contravantuiri disipative echipate cu amortizoare cu fluid nano-micro magnetoreologic – SEMNAL-MRD – Seismic protection of engineering structures through dissipative braces of nanomicro magnetorheological fluid dampers", coordinated by Politehnica University of Timisoara (coordinator Dan Dubina). This particular research contract is supported by a strong industrial interest, which motivates an applicative output of the research. Semi-active control has an important potential in seismic protection of buildings, as it can adapt to the characteristics of the future seismic events, unknown at the design stage. Moreover, the device can adapt its characteristics to the requirements imposed by different design situation (serviceability vs. ultimate limit state, earthquake vs. wind loading). Semi-active structural control has a strong interdisciplinary character. This kind of research opens the possibility of enlarging the research network, and accessing new funding sources. It is intended in the future to enlarge the research partnership and apply for a Horizon 2020 project, in order to extend the obtained results from proof-of-concept to application-ready stage.

**"Improved seismic design criteria for steel structures in case of ground motions with high frequency content in the long-period range"** is another subject that deserves attention. Ground motions characterised by large control periods $T_C$ impose substantially larger demands on structures responding in the inelastic range than the ones with small control periods. In the former case conventional design should be based on reduced behaviour factors. Though this is a well-known fact, modern seismic design codes disregard it. The problem is especially important in the case of Romania, where specific characteristics of Vrancea seismic source and soft soil conditions generate ground motions with large values of control periods ($T_C$ = 1,6 sec) in Bucharest area. This situation is quite unusual, and therefore did not receive much attention globally. A systematic numerical program is necessary in order to evaluate the seismic performance for a relevant set of buildings and derive behaviour factors to be introduced in future revisions of national seismic design code and Eurocode 8.

Seismic performance of steel structures depends to a large extent on the behaviour of its connections. A great deal of research was devoted to analysis of cyclic response of various typologies of beam to column connections in moment resisting frames worldwide. Design guidelines for prequalified beam to column connections exist in United States and Japan. A comprehensive research project with the same target is underway in Europe (EQUALJOINTS project, see section 0). However, connections in steel concentrically braced frames received much less attention. Design guidelines for brace connections in seismic resistant construction are virtually non-existent in Europe. A European (RFCS) project devoted to this subject can provide the framework for filling this gap. **"Design criteria for connections in concentrically braced frames and prequalification of typical European connections"** is thus another subject that the author wishes to develop in the future.

All of the subjects addressed to date by the author are strongly biased toward the applicative and deterministic components of seismic engineering. Though future research directions in view will remain focused on this approach, the large uncertainty which characterises seismic action and the uncertainties in modelling of structural response ask for a probabilistic treatment of the problem. Therefore, **"seismic vulnerability and risk assessment"** will complete the list of research directions that the author wishes to explore in the future.

The complexity of today's research, its multidisciplinary character, and the demand for applicative outputs ask for a collaborative approach in its implementation. Therefore one of the main aspects of the professional development plan consists in strengthening existing connections with international and national research partners. At the European level, the author intends to continue and develop his scientific collaboration with University of Naples Federico II, Technical Research Centre of Finland VTT, University of Ljubljana, Joint Research Centre in Ispra, University of Coimbra, Imperial College London. Initiation of new collaborations with Budapest University of Technology and Economics, and University of Porto is also envisaged.

At the same time, collaboration at the national level is considered to be important. Existing connections with Technical University of Civil Engineering in Bucharest and the Technical University of Cluj-Napoca will be maintained and developed. It is intended to create new connections at the Gheorghe Asachi Technical University of Iasi. The experimental infrastructure from the Politehnica University of Timisoara, specialised in quasi-static tests and potentially pseudo-dynamic ones is complementary to the shaking table testing available at Technical University of Iasi. Collaboration between the two research facilities is believed to be synergetic and mutually beneficial, and therefore is on the list of future developments of the author.

Collaboration with industrial partners will be maintained and developed as well. Past experience with design companies and steel producers (Popp & Asociatii, Bucharest and Hidromatic system, Timisoara) has shown that this collaboration is effective in identifying innovative solutions to practical problems and attracting funding for research.

A more active engagement in the activities of the technical committees of the European Convention for Constructional Steelwork (ECCS), the European Committee for Standardization (CEN) and Romanian Standards Association (ASRO) is also envisaged. Currently CEN/TC250 received a mandate for developing the second generation of structural Eurocodes. The author intends to contribute to this process, both by applying for the role of project team member in tasks related to seismic design of steel structures, as well as through the reviewing activity of CEN and ASRO technical committees.

The author will continue to seek funding of the research activities through more active involvement in grant applications. European funding opportunities, like the Research fund for Coal and Steel and Horizon 2020 will be emphasised.

Improvement of the research infrastructure (experimental, computing and software) will continue to be addressed, through allocating resources within research grants, but also by seeking infrastructure-specific funding opportunities. At the same time, the internal organisation of the laboratory will be improved, by setting up a set of procedures for performing tests, maintenance of equipment, and archiving of experimental results.

Academic activities are regarded as an important part of the personal development plan. The primary objective in this area consists in earning the right to conduct PhD tesis, and subsequently to effectively coordinate PhD students. The subjects to be investigated would be those stated in section 3.1 "Scientific development plan", and will be supported by research grants.

Another direction followed will be the improvement of the teaching methods and aids. Though the author has already prepared lecture notes for the courses he teaches, some of them can benefit from better teaching materials. In particular, it is intended to write two books on "Basis of structural design" and "Performance based earthquake engineering", supporting the corresponding lectures. On the other hand, the teaching methods will be improved by involving the students through interactive learning techniques. In particular, laboratory activities demonstrating the dynamic response of structures using the shaking table will be organised with students participating to the course of "Structural dynamics and earthquake engineering". At the same time, the author intends to develop web-based applications demonstrating different dynamic phenomena, which will increase attractiveness of the course and improve student's comprehension.

Further development of the international cooperation at the academic level is also targeted. As a concrete measure, the author intents to coordinate new student and teaching staff exchange through the ERASMUS+ scheme. As a first step, an application for a cooperation agreement with the Technical University of Moldova is intended to be established.

Last but not least, the continuing education is an area that is relatively underdeveloped currently and which has a good potential for improvement. Considering the fact that design codes are in a permanent process of improvement and revision, and that research outcomes should find their way into practice, there is an increasing demand for short-term training courses for practicing engineers. The author intends to play an active role in organisation such courses in cooperation with the Romanian Association of Structural Engineering (AICPS).

# 4 REFERENCES

Abaqus. "Analysis User's Manual". Dassault Systèmes Simulia Corp., Providence, Rhode Island, U.S.A.

AISC (2005). "Seismic Provisions for Structural Steel Buildings". American Institute of Steel Construction, Inc. Chicago, Illinois, USA.

Akiyama H. (1999). Behaviour of connections under seismic loads. Control of semi-rigid behaviour of civil engineering structural connections. COST C1. Proceedings of the international conference, Liege, 17-19 September 1998.

Akkar, S., Sandıkkaya, M. A., Şenyurt, M., Azari Sisi, A., Ay, B. Ö., Traversa, P., Douglas, J., Cotton, F., Luzi, L., Hernandez, B., and Godey, S. (2014). "Reference database for seismic ground-motion in Europe (RESORCE)." Bulletin of Earthquake Engineering, 12(1), 311–339.

Ali A.M., Farid B.J., and Al-Janabi A.I.M. (1990). "Stress-strain relationship for concrete in compression made of local materials", JAU: Eng. Sci., Vol. 2, pp 183-194.

ANSI/AISC 341 (2010). "Seismic provisions for structural steel buildings". American Institute of Steel Construction, Chicago, Illinois; 2010.

ANSI/AISC 358-05 (2005), "Prequalified Connections for Special and Intermediate Steel Moment Frames for Seismic Applications", American Institute of Steel Construction.

Astaneh-Asl A. (2001). Seismic Behavior and Design of Steel Shear Walls, Steel TIPS, USA.

Beck H. (1999). "Nailed shear connection in composite tube columns", Second European Conference on Steel Structures, Prague, 26-29 May 1999, pp. 565–568.

Beck H. (2010). "Nailed shear connection in composite tube column with Hilti X-DSH 32 P10 – Installation instructions for test samples at University of Timisoara", Hilti AG., 22.11.2010.

Beck H., Reuter M. (2005). "Powder actuated fasteners in steel construction", Steel Construction Calendar 2005 - Stahlbau Kalender 2005 (http://www.us.hilti.com/fstore/holus/LinkFiles/Stahlbaukalender.pdf)

Bordea S., Stratan A. Dubina D. (2008). "Performance based evaluation of a non –seismic RC frame strengthened with Buckling Restrained Braces". Urban Habitat Constructions under catastrophic events, COST Action C26, Ed. Mazzolani F. M. et al.

Chi, H., and Liu, J. (2012). "Seismic behavior of post-tensioned column base for steel self-centering moment resisting frame." Journal of Constructional Steel Research, 78, 117–130.

Chung, K.F. and Lau, L., "Experimental Investigation on Bolted Moment Connections Among Cold Formed Steel Members", Engineering Structures, 1999, Vol. 21, No. 10, pp. 898-911.

Danku, G., 2011. Study of the development of plastic hinges in composite steel-concrete structural members subjected to shear and/or bending. PhD thesis. Politehnica University of Timisoara.

Dubina, D., Stratan, A., and Dinu, F. (2008). "Dual high-strength steel eccentrically braced frames with removable links." Earthquake Engineering and Structural Dynamics, 37(15), 1703–1720.

Dubina, D., Stratan, A., Bordea, S. (2007). "Seismic Retrofit of r.c. frames with hysteretic bracing". Steel and Composite Structures, Ed. Y.C. Wang and C.K. Choi, Taylor and Francis, London, UK, p. 833 – 840.

Dubina, D., Stratan, A., Ciutina, A., Fulop, L., Nagy, Zs., "Performance of Ridge and Eaves Joints in Cold-formed Steel Portal Frames", Proc. of the 17th int. Specialty Conf., Orlando, Florida, USA, 04-05 Nov. 2004, Univ. of Missouri-Rolla, Ed. R.A. LaBoube, W-W. Yu, pp. 727-742.

Dubina, D., Vulcu, C., Stratan, A., Ciutina, A., Grecea, D., Ioan, A., Tremeea, A., Braconi, A., Fülöp, L., Jaspart, J.-P., Demonceau, J.-F., Hoang, L., Comeliau, L., Kuhlmann, U., Kleiner, A., Rasche, C., Landolfo, R., D'Aniello, M., Portioli, F., Beg, D., Cermelj, B., Može, P., da Silva, L. S., Rebelo, R., Tenchini, A., Kesti, J., Salvatore, W., Caprili, S., and Ferrini, M. (2015). High strength steel in seismic resistant building frames (HSS-SERF). Research Fund for Coal and Steel, Final report, European Commission, B-1049 Brussels, 181.

Dundu, M., Kemp, A.R., "Strength Requirements of Single Cold Formed Channels Connected Back-to-back", Journal of Constructional Steel Research, 2006, Vol. 62, Issue 3, pp. 250-261.

Dutta A., Dhar S., Acharyya S.K. (2010). "Material characterization of SS 316 in low-cycle fatigue loading", Journal of Materials Science, Vol. 45, Issue 7, pp. 1782-1789.

ECCS (1985). "Recommended Testing Procedure for Assessing the Behaviour of Structural Steel Elements under Cyclic Loads", European Convention for Constructional Steelwork, TWG 13 Seismic Design, Report No. 45, 1985

EN 10025-2: 2004, Hot rolled products of non-alloy structural steels, Technical delivery conditions for non-alloy structural steels.

EN 10025-6: 2004, Hot rolled products of non-alloy structural steels, Technical delivery conditions for flat products of high yield strength structural steels in the quenched and tempered condition.

EN 10210-2 (2006). "Hot finished structural hollow sections of non-alloy and fine grain steels - Part 2: Tolerances, dimensions and sectional properties". CEN - European Committee for Standardization.

EN 1990 (2001). "Eurocode 0: Bases of structural design". CEN - European Committee for Standardization.

EN 1991 (2002). "Eurocode 1: Actions on structures - Part 1-1: general actions, densities, self-weight, imposed loads for buildings". CEN - European Committee for Standardization.

EN 1993-1-1 (2005). "Eurocode 3, Design of steel structures - Part 1-1. General rules and rules for buildings". European Committee for Standardization – CEN.

EN 1993-1-3. "Eurocode 3: Design of Steel Structures. Part 1-3: General Rules. Supplementary Rules for Cold-formed Thin Gauge Members and Sheeting", European Committee for Standardization, 2001.

EN 1993-1-8 (2005). "Eurocode 3: Design of Steel Structures - Part 1-8: Design of joints", CEN - European Committee for standardization.

EN 1994-1-1 (2004). "Eurocode 4: Design of composite steel and concrete structures - Part 1-1: General rules and rules for buildings". CEN - European Committee for Standardization.

EN 1998-1 (2004). "Eurocode 8: Design of structures for earthquake resistance. Part 1: General rules, seismic actions and rules for buildings". CEN - European Committee for Standardization.

EN 15129 (2009). "Anti-seismic devices". CEN - European Committee for Standardization.

European pre-QUALified steel JOINTS – EQUALJOINTS, RFSR-CT-2013-00021, project website: http://dist.dip.unina.it/2013/12/09/equaljoints/

FEMA 356 (2000). "Prestandard and commentary for the seismic rehabilitation of buildings", Federal Emergency Management Agency, Washington (DC).

FIB Bulletin 14 (2001). "Externally bonded FRP reinforcement for RC structures".

Fink A. (1997). "Das Momentenrotationsverhalten von Verbundknoten mit Verbundstützen aus Rechteckhohlprofilen", Diploma-work, Institute for Steel and Timber Structures, University of Innsbruck.

Hanswille G., Beck H., Neubauer T. (2001). "Design concept of nailed shear connections in composite tube columns", Proceedings of the International Symposium on Connections between Steel and Concrete, RILEM Publications SARL, Print-ISBN: 2-912143-25-X, e-ISBN: 2351580346, Stuttgart, Germany, September 10-12, pp. 1056-1065.

Herning, G., Garlock, M. E. M., and Vanmarcke, E. (2011). "Reliability-based evaluation of design and performance of steel self-centering moment frames." Journal of Constructional Steel Research, 67(10), 1495–1505.

Hilti AG (1998). Prüfbericht nr. 172268, Prüfobjekt: Hilti Nägel X-DSH 32 P10 Special, Auftragsnummer 555236, 25-27.05.1998.

Hilti-Catalogue (2005). "Design Manual, Anchor Technology".

Huber G. (2001). "Semi-continuous beam-to-column joints at the Millennium Tower in Vienna, Austria", Steel and Composite Structures, Vol. 1, No. 2, pp. 159-170.

IAEE/NICEE (2004). "Guidelines for earthquake resistant non-engineered construction", First printed by International Association for Earthquake Engineering, Tokyo, Japan. Reprinted by the National Information Center of Earthquake Engineering, IIT Kanpur, India.

Iyama, J., Kuwamura, H. (1999). Probabilistic advantage of vibrational redundancy in earthquake-resistant steel frames. Journal of Constructional Steel Research, 52: 33-46.

Jaspart, J.P., Steenhuis, M., Anderson, D. (1998). "Characterisation of the Joint Properties by Means of the Component Method", Control of Semi-rigid Behaviour of Civil Engineering Structural Connections, COST C1, Proc. of the Int. Conf, Liege, 17-19 September 1998.

KELLY, T.E. (2001). "Design Guidelines", Holmes Consulting Group, www.holmesgroup.com

Kiggins, S., and Uang, C.-M. (2006). "Reducing residual drift of buckling-restrained braced frames as a dual system." Engineering Structures, 28(11), 1525–1532.

Korotkov V., Poprygin D., Ilin K., Ryzhov S. (2004). "Determination of dynamic reaction in concrete floors of civil structures of nuclear power plant in accidental drops of heavy objects", ABAQUS Users' Conference, Boston 25-27 May, 2004, pp. 399-408.

Kwon, Y.B., Chung, H.S., and Kim, G.D. (2006). "Experiments of Cold-formed Steel Connections and Portal Frames", Journal of Structural Engineering, Vol. 132, No. 4, pp. 600-607.

Landolfo, R., D'aniello, M, Portioli, F. (2010). "Simulation of inelastic cyclic behaviour of steel concentric bracings", 14ECEE, Ohrid, T3, paper no.1816.

Larcher T.Z. (1997). "Versuche zur Krafteinleitung der Trägerauflagerkräfte bei Hohlprofilverbundstützen mit Setznägeln", Diploma-work, Institute for Steel and Timber Structures, University of Innsbruck.

Lim, J.B.P. (2001). "Joint Effects in Cold-formed Steel Portal Frames", University of Nottingham, Ph.D. Thesis.

Lim, J.B.P. and Nethercot, D.A. (2003). "Ultimate Strength of Bolted Moment-connections between Cold-formed Members", Thin-Walled Structures, Vol. 41, No. 11, pp. 1019-1039.

Lim, J.B.P. and Nethercot, D.A. (2004). "Stiffness Prediction for Bolted Moment-connections between Cold-formed Steel Members", Journal of Constr. Steel Res., Vol. 60, Issue 1, pp. 85-107.

List of tallest buildings in Bucharest. (2015). In Wikipedia, The Free Encyclopedia. Retrieved May 3, 2015.

Maris C., Vulcu C., Stratan A., Dubina D. (in print). "Validation Through Numerical Simulations of the Design Procedure for Bolted Beam–to-Column Connections with Haunches", Pollack Periodica, Budapest, Hungary.

Mazzolani F.M. (2006). "Seismic upgrading of RC buildings by advanced techniques". The ILVA – IDEM Research Project, Polimetrica International Scientific Publisher.

NEHRP (2003). NEHRP Recommended provisions for new buildings and other structures (FEMA 450). Part 1: Provisions and Part 2: Commentary. Building Seismic Safety Council, National Institute of Building Sciences, Washington, D.C.

P100-1 (2006). Seismic design code P100: Part I: Design rules for buildings (in Romanian).

PANAIT, A., ŞERBAN, V., ANDRONE, M., CIOCAN, G.A., ZAMFIR, M. (2007). "Metoda ŞERB - SITON pentru controlul, limitarea si amortizarea miscarilor seismice a structurilor metalice", a X-a ediţie a Zilelor Academice Timisene: Structuri metalice amplasate in zone seismice. Preocupari actuale, 25 mai 2007.

Park, R. and Paulay, T. (1975). "Reinforced Concrete Structures", New Zealand, John Wiley & Sons, Inc., New York.

Rai D.C. (2000). "Future trends in earthquake-resistant design of structures", Current Science, volume 79, number 9.

Ricles J.M., Popov E.P. (1994). Inelastic link element for EBF seismic analysis. ASCE, Journal of Structural Engineering, 1994, Vol. 120, No. 2: 441-463.

Roke, D., and Jeffers, B. (2011). "Parametric study of self-centering concentrically-braced frame systems with friction-based energy dissipation." Behaviour of Steel Structures in Seismic Areas, CRC Press, 691–696.

Seismosoft (n.d.) "SeismoStruct– A computer program for static and dynamic nonlinear analysis of framed structures," available from http://www.seismosoft.com.

Silva L.S., Rebelo C., Serra M., Tenchini A. (2011), "Selection of structural typologies and design of optimized dual-steel multi-storey frames", Mid Term Report HSS-SERF Project: "High Strength Steel in Seismic Resistant Building Frames", Grant N0 RFSR-CT-2009-00024.

Stratan A., Ioan A., Dubina D., Poljanšek M., Molina J., Pegon P., Taucer F. (2015). "Large-scale tests on a re-centring dual eccentrically braced frame", The 8th International Conference on Behaviour of Steel Structures in Seismic Areas (STESSA'15), 1-3 July, Tongji University, Shanghai, China;

Stratan, A., (2003). "Studiul comportării clădirilor multietajate cu cadre metalice duale amplasate în zone seismice". Universitatea Politehnica Timişoara, 324 pag.

Stratan, A., and Dubina, D. (2004). "Bolted links for eccentrically braced steel frames." Proc. of the Fifth AISC / ECCS International Workshop "Connections in Steel Structures V. Behaviour, Strength and Design," Delft University of Technology, The Netherlands, 223–232.

Stratan, A., Ioan, A., Dubina, D., Taucer, F., Poljanšek, M., Molina, J., Pegon, P., D'Aniello, M., and Landolfo, R. (2014). "Experimental program for large-scale tests on a re-centring dual eccentrically braced frame." 7th European Conference on Steel and Composite Structures EUROSTEEL 2014, European Convention for Constructional Steelwork, ECCS, Napoli, Italy, paper no. 37–300, 8 p.

Tremblay, R. (2002). "Inelastic seismic response of steel bracing members." Journal of Constructional Steel Research, 58, 665–701.

Vargas, R. and Bruneau, M. (2006). Seismic design of multi-story buildings with metallic structural fuses. Proceedings of the 8th U.S. National Conference on Earthquake Engineering, April 18-22, 2006, San Francisco, California, USA. Paper No. 280.

Vargas, R., and Bruneau, M. (2006). "Seismic design of multi-story buildings with metallic structural fuses." Proceedings of the 8th US National Conference on Earthquake Engineering (Paper N. 280), San Francisco, California, USA, 18–22.

Yu, W.K., Chung, K.F. and Wong, M.F. (2005). "Analysis of Bolted Moment Connections in Cold-formed Steel Beam–column Sub-frames", Journal of Constructional Steel Research, Vol. 61, Issue 9, pp. 1332-1352.

Ziemian, R.D. (2010). "Guide to Stability Design Criteria for Metal Structures". Sixth edition. John Wiley & Sons, Inc., USA.